Molecular Physics
Vol. 108, Nos. 7–9, 10 April–10 May 2010, 827–846

Taylor & Francis
Taylor & Francis Group

INVITED ARTICLE

Accurate level energies in the $EF^1\Sigma_g^+$, $GK^1\Sigma_g^+$, $H^1\Sigma_g^+$, $B^1\Sigma_u^+$, $C^1\Pi_u$, $B'^1\Sigma_u^+$, $D^1\Pi_u$, $I^1\Pi_g$, $J^1\Delta_g$ states of H_2

D. Bailly[a], E.J. Salumbides[b]†, M. Vervloet[c] and W. Ubachs[b]*

[a]*Laboratoire Photophysique Moléculaire, Université de Paris-Sud, Orsay, France;* [b]*Laser Centre, Vrije Universiteit, De Boelelaan 1081, 1081 HV Amsterdam, The Netherlands;* [c]*Synchrotron Soleil, L'orme des Merisiers, Saint-Aubin BP 48, 91192 Gif-sur-Yvette, France*

(*Received 22 July 2009; final version received 5 October 2009*)

By combining results from a Doppler-free two-photon laser excitation study on several lines in the $EF^1\Sigma_g^+ - X^1\Sigma_g^+$ (0,0) band of H_2 with results from a Fourier-transform spectroscopic study on a low-pressure discharge in hydrogen, absolute level energies, with respect to the $X^1\Sigma_g^+$, $v=0$, $N=0$ ground level, were determined for 547 rovibronically excited states in H_2. While for some of the levels in the $EF^1\Sigma_g^+$ and $B^1\Sigma_u^+$ states the uncertainties are as low as $0.0001\,cm^{-1}$, the accuracy of other levels is lower. The general improvement in the accuracy for the comprehensive data set of level energies is by an order of magnitude with respect to previous measurements. An updated listing of transition wavelengths of the spectral lines in the Lyman and Werner bands is presented, based on combination differences between the presently obtained $B^1\Sigma_u^+$ and $C^1\Pi_u$ level energies and those in the $X^1\Sigma_g^+$ ground state.

Keywords: molecular hydrogen; Fourier transform spectroscopy; extreme ultraviolet; proton–electron mass ratio; accurate level energies

1. Introduction

The hydrogen molecule is the smallest neutral molecular system and therewith a benchmark system in spectroscopy and quantum *ab initio* calculation of molecular structure. It has been the subject of numerous investigations over many decades. The discovery of hydrogen might be ascribed to Cavendish as early as 1766 [1]. From the reactions of different acids with metals he obtained a gas that burns with a blue flame, producing water. He conjectured that this gas was *phlogiston*, the elusive carrier of fire, which was still believed to be some unique substance at that time. Lavoisier [2] gave the gas its name *hydrogen*, Greek for *water former*, after his successful decomposition of water into hydrogen and oxygen; he therewith identified hydrogen as an element. On the basis of Gay-Lussac's law of multiple proportions [3] Avogadro showed that molecules of elementary hydrogen consist of two atoms, as molecules of many other gaseous elements [4]. As early as 1865 Plücker and Hittorf [5] measured, in addition to the Balmer lines, several spectral lines in the visible range; these were referred to as the 'second spectrum' of hydrogen. The open structured spectrum was difficult to classify and its origin was a subject of controversy for many years. In the debate over the second spectrum it was contended that a substance could have only one spectrum. Fulcher managed finally to arrange the lines, the number and accuracy of which had grown due to the activity of many researchers, into a Deslandres band scheme, showing that the second spectrum had the signature of a molecular band structure [6]. But at the time that this issue was settled, the VUV-spectroscopic work of Lyman [7] already had set the scene for an unambiguous spectrum of the hydrogen molecule.

Early but comprehensive accounts of the hydrogen spectrum are given in the book by Richardson [8] and in the *Dieke atlas* [9]. These manuscripts contain a wealth of data that still have not been analysed in their entirety with many lines remaining unassigned. A general feature of the H_2 spectrum is that the $X^1\Sigma_g^+$ ground electronic state is separated from the manifold of excited states by a large energy gap: hence, the entire electronic absorption spectrum is in the region of the extreme ultraviolet, at wavelengths $\lambda < 110\,nm$, and the emission spectrum involving the electronic ground

*Corresponding author. Email: wimu@nat.vu.nl
†Current Address: Department of Physics, University of San Carlos, Cebu, Philippines.

ISSN 0026–8976 print/ISSN 1362–3028 online

DOI: 10.1080/00268970903413350
http://www.informaworld.com

state is in the range of the vacuum ultraviolet $\lambda = 100$–160 nm. In these wavelength ranges it is difficult to perform precision studies for a determination of accurate level energies of the excited states. Progress was made nevertheless, through the use of large classical spectrometers, by Herzberg and Howe [10], culminating in the combined emission and absorption study of the Lyman and Werner bands by Dabrowski [11]. Later, the hydrogen vacuum-ultraviolet emission spectrum was reinvestigated at the Meudon Observatoire, resulting in an atlas of spectral lines by Roncin and Launay [12], a listing of tables of spectral lines of the Lyman bands [13] and of the Werner bands [14], and a derivation of rovibronic level energies for the $B^1\Sigma_u^+$ and $C^1\Pi_u$ states [15].

With the development of tunable lasers sources in the extreme ultraviolet wavelength range further improvement was made on the accuracy of lines in the $B^1\Sigma_u^+$ and $C^1\Pi_u$ electronic systems. (These are the strongest electronic absorption systems in molecular hydrogen, hence these are readily observed in many astrophysical objects.) A first investigation, using a tunable laser, based on a grating-based oscillator, led to a slight improvement on the transition wavelengths [16,17], while in second instance implementation of injection-seeding, pulsed-dye-amplification, and molecular beam techniques yielded improvement by another order of magnitude [18].

Transitions between different electronically excited states can be observed in the visible wavelength range, allowing for much higher precision. In fact Dieke focused on this approach. From this perspective, the H_2 molecule has a spectrum that is difficult to interpret. The line assignment is greatly hampered by the fact that rotational and vibrational splittings are of the same order as the electronic separations, to the extent that the typical molecular band structure is fully lost and a random-like spectrum results. Assignments based on *ab initio* calculations are further hampered by the strong non-Born–Oppenheimer effects in the hydrogen molecule, due to its low mass. For this reason a large fraction of the lines in the *Dieke atlas* are still unassigned.

The excited states of hydrogen have been the subject of much theoretical work. For the *gerade* states considered here the most relevant theoretical studies are the high-level non-adiabatic *ab initio* calculations of Yu and Dressler [19] and the multi-channel quantum defect (MQDT) calculations of Ross and Jungen [20]. Both those works, published in 1994, compare their calculated term values with experiment, with Yu and Dressler also summarising the results of new assignments of lines from the *Dieke atlas* in presenting their experimentally determined level energies. For the *ungerade* states considered here similar work is seen in the non-adiabatic ab initio calculations of Senn *et al.* [21] and the earlier MQDT calculations of Jungen and Atabek [22].

At this point we briefly mention the difference between the approaches to determine level energies in first principle calculations. The first method starts with an *ab initio* calculation of potential energy curves in the framework of the Born–Oppenheimer (BO) approximation, hence for infinite nuclear masses. Variational methods and large basis sets of Hylleraas-type wave functions are used to solve the Schrödinger equation. This method was pioneered for the hydrogen molecule by Kolos and Wolniewicz [23]. Subsequently the so-called adiabatic corrections are calculated, non-BO mass-dependent effects that can still be expressed in terms of a potential; in a vector representation of all electronic eigenstates, their contributions are on the diagonal of the coupling matrix. In a third step the so-called non-adiabatic corrections are calculated that represent couplings between electronic states off-diagonal in the coupling matrix. In calculating these corrections the terms are evaluated, which were left out of the zero-order BO-Hamiltonian. In a final step level energies are calculated via the method of Coupled Schrödinger Equations (CSE) using the adiabatic potentials and the off-diagonal matrix elements. This route has been worked out by Dressler and co-workers deriving level energies for states of *gerade* symmetry [19] and of *ungerade* symmetry [21]. The achieved accuracy for excited states is typically some few $0.1\,\mathrm{cm}^{-1}$ for low vibrational quantum numbers up to several cm^{-1} for higher lying states. For the specific case of the $X^1\Sigma_g^+$ ground electronic state, not subject of our present investigation, Wolniewicz perfected this method to obtain an accuracy of $0.001\,\mathrm{cm}^{-1}$ [24]. The method also yields the wave function composition of each level on a mixed basis, which may be used for level identification.

In the MQDT formalism quantum defect functions are derived from the potential energy curves, and as Jungen and Atabek have shown [22] for the specific case of the lowest states of *ungerade* symmetry, there is no need for explicit calculations of adiabatic and non-adiabatic corrections since the vibronic coupling arises via frame tranformations in the unified treatment of MQDT. The resulting level energies reach similar accuracies as via the CSE method. The CSE method was further developed by the Meudon group [15,25]; in order to better reproduce the experimental data on the level energies in the $B^1\Sigma_u^+$ and $C^1\Pi_u$ states [12–14] the potential energy functions were adapted in fitting routines. The latter method is therefore

semi-empirical rather than first principles; accuracies achieved by this method are typically few 0.10 cm^{-1}.

The quest for detection of a possible variation of fundamental constants, and the important role of the spectrum of molecular hydrogen therein [26,27], motivated a reinvestigation of the H_2 spectrum with the goal of determining level energies and wavelength positions at the highest possible accuracy. It was realised that the most accurate excited-state level energies can be determined in a two-step approach [28]. In a first step, anchor levels in the $EF^1\Sigma_g^+$ system are determined via accurate two-photon laser spectroscopy [29]. In a second step precision Fourier Transform spectroscopy within the manifold of electronically excited states is performed to determine level energies with respect to the anchor levels. This work builds and improves upon the previous FT-studies of Herzberg and co-workers [30,31]. The extensive FT reinvestigation of H_2 has first led to an analysis of some triplets states [32]; now the same spectrum is used to analyse the $EF^1\Sigma_g^+ - B^1\Sigma_u^+$, $EF^1\Sigma_g^+ - C^1\Pi_u$, $GK^1\Sigma_g^+ - B^1\Sigma_u^+$, $GK^1\Sigma_g^+ - C^1\Pi_u$, $I^1\Pi_g - C^1\Pi_u$, $D^1\Pi_u - EF^1\Sigma_g^+$, $B'^1\Sigma_u^+ - EF^1\Sigma_g^+$, $H^1\Sigma_g^+ - B^1\Sigma_u^+$, $H^1\Sigma_g^+ - C^1\Pi_u$, $I^1\Pi_g - B^1\Sigma_u^+$, $J^1\Delta_g - B^1\Sigma_u^+$, $J^1\Delta_g - C^1\Pi_u$ systems over a wide range of wavelengths. In combination with the determination of anchor levels, this yields accurate *absolute* level energies of a large number of rovibrational levels in these electronic states, with respect to the $X^1\Sigma_g^+$ ground state. An improvement of at least an order of magnitude is achieved over previous studies. It is the purpose of the present paper to present these accurately determined level energies.

2. Experimental

The experimental determination of excited state level energies is based on two completely independent measurements. Two anchor lines in the $EF^1\Sigma_g^+$ manifold are determined by two-photon spectroscopy. A highly sophisticated measurement scheme employing Doppler-free two-photon ionisation [29], using a home-built narrowband pulsed titanium-sapphire laser with on-line recording of frequency chirp, absolute frequency calibration against a frequency comb laser [33], and Sagnac-interferometric alignment of counter-propagating laser beams [34]. A typical example of a spectrum of the EF – X (0,0) Q(3) line is shown in Figure 1. The transition energies of Q(0)–Q(5) in the EF – X (0,0) band obtained from the high-resolution two-photon spectroscopy [28,29] are listed in Table 1. These two-photon experiments yield highly accurate level energies for two anchor levels in H_2: the $EF^1\Sigma_g^+$, $v=0$, $N=0$ level at 99164.78691 (11) cm^{-1} is the anchor level for para-hydrogen, while $EF^1\Sigma_g^+$, $v=0$, $N=1$ level at 99228.21823 (19) cm^{-1} is the anchor level for ortho-hydrogen [28]. The entire framework of excited states in H_2 is further built up with respect to these two values. The transition energies of Q(2)–Q(5) are used in the assessment and verification of the combination method described below. Figure 2 shows the potential energy diagram of H_2 with the relevant states probed in the present study [35].

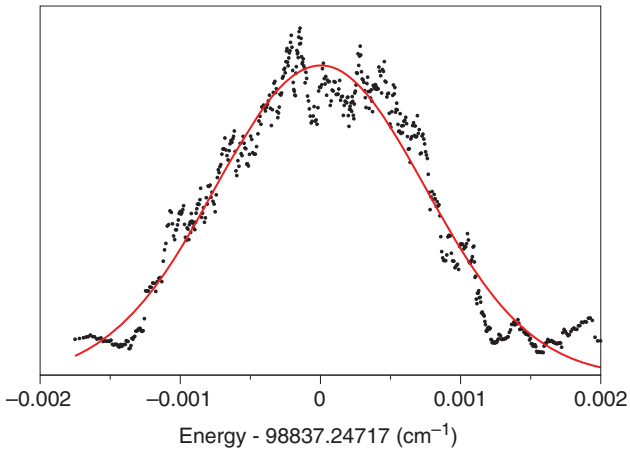

Figure 1. Spectral recording of the Q(3) line in the $EF^1\Sigma_g^+ - X^1\Sigma_g^+$ (0,0) band using Doppler-free two-photon spectroscopy with counter-propagating laser beams in the deep ultraviolet.

Table 1. Transition energies of the EF – X (0,0) Q branch obtained from high-precision deep UV spectroscopy.

N	Energy cm^{-1}
0	99164.78691 (11)
1	99109.73139 (18)
2	99000.18301 (11)
3	98837.24717 (15)
4	98622.52699 (10)
5	98358.07138 (15)

In a second independent experiment, a Fourier transform emission study is performed revealing a multitude of mutually overlapping band systems over an enormous wavelength interval ranging from 450 nm in the blue to 5 μm in the infrared.

The experimental technique used here has been used previously [32] and is only briefly described. A microwave discharge (2450 MHz) was established in a low pressure of molecular hydrogen flowing through a quartz tube (diameter: 1 cm, length: 25 cm) at moderate speed by means of a 20 m^3/h mechanical pump. The power of the discharge (about 70 W) and

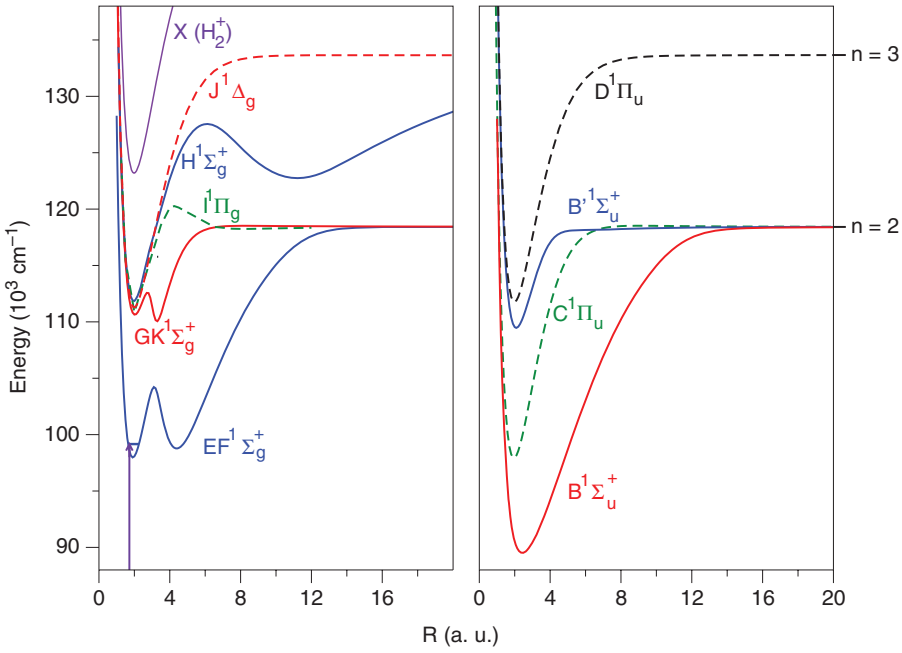

Figure 2. Potential energy diagram of the relevant states probed: states of *gerade* symmetry on the left, and states of *ungerade* symmetry on the right. The potentials are obtained from [35].

the gas pressure (about 5 mbar) were adjusted in order to obtain a maximum ratio of the molecular/atomic hydrogen optical emission and to provide optimum stability and intensity of the emitted light. The emission spectrum was recorded from 1800 to 22500 cm^{-1} by using appropriate coloured or interference optical filters and detectors. As for detectors we used a liquid nitrogen cooled InSb photodiode for the range 1800–6500 cm^{-1} (equipped with a cold short wavelength pass interference filter for the range 3300–6500 cm^{-1}), a liquid nitrogen cooled InGaAs photodiode (for 6500–9000 cm^{-1}), an avalanche silicon photodiode (9000–17,000 cm^{-1}) and a photomultiplier (17,000–22,500 cm^{-1}). An overview spectrum of the entire recorded region is shown in Figure 3. The spectrum was recorded at Doppler limited resolution, varying from about 0.02 cm^{-1} (infrared) to 0.2 cm^{-1} (violet). Figure 4 shows two 15 cm^{-1} parts of the spectrum in the infrared and visible regions where it can be easily noted that, for this spectrum, the peak determinations will be more accurate in the infrared than in the visible range. Traces of CO or Ar, for which the line frequencies are reported in [36] and [37] respectively, were added to the hydrogen flow for calibration purposes. The spectrum consists of a total of 61 records. Each record displays one of the four spectral ranges mentioned above and results in the Fourier transform of 100 to 1000 co-added interferograms.

The rotational analysis was carried out with the help of the published results of Dieke [9] and

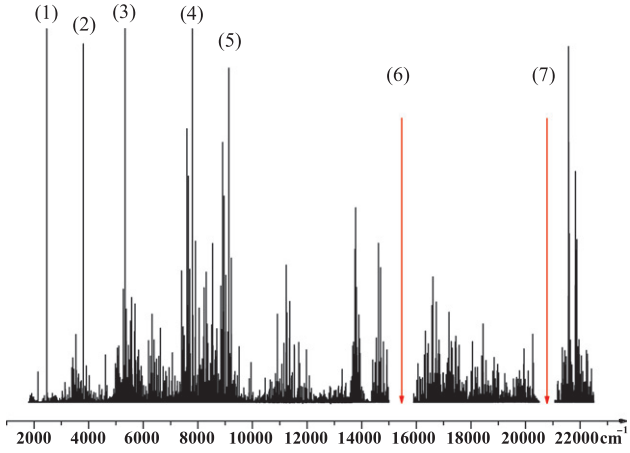

Figure 3. Overview of the entire Fourier transform emission spectrum obtained from 2000 to 22,000 cm^{-1}. The very strong and saturated lines are atomic lines: (1) Brackett-α; (2) Brackett-β; (3) Paschen-α; (4) Paschen-β; (5) Paschen-γ. The two ranges without records correspond to the atomic line Balmer-α (6) and Balmer-β (7).

Dabrowski [11] and was guaranteed by using primarily the well known technique of combination differences. First, the analysis was focused on the bands of the system $EF^1\Sigma_g^+$ ($v=0$) – $B^1\Sigma_u^+$ (v), resulting in a set of precise combination differences in $EF^1\Sigma_g^+$ ($v=0$). Then, it was followed by an extensive analysis of the entire $EF^1\Sigma_g^+ - B^1\Sigma_u^+$ system, leading to an increased number of the set of combination differences for each vibrational level of one particular electronic state, or

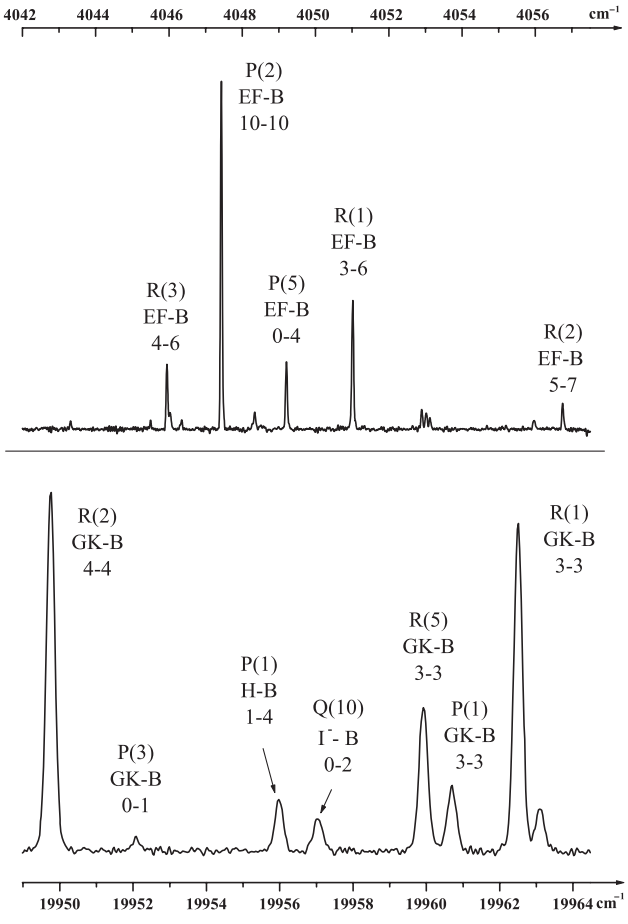

Figure 4. Detail spectra of two spectral ranges covering 15.5 cm^{-1}: (a) in the blue spectral region, and (b) in the infrared region. The spectra clearly show the different Doppler-limited resolution for the FT-emission spectrum in both regions.

between ro-vibrational states of the two different electronic states, as shown in Figure 5. At this stage, a preliminary set of energies for the levels involved in the combination differences set was established, taking as anchor energies the very precise values of the levels $N=0$ (para H_2) and $N=1$ (ortho H_2), $EF^1\Sigma_g^+$ ($v=0$) determined by two-photon laser spectroscopy [28]. Afterwards, the determination of the combination differences and level energies was extended to the levels of the $GK^1\Sigma_g^+$, $H^1\Sigma_g^+$, $I^1\Pi_g$ and $J^1\Delta_g$ states by analysing the systems GK – B, H – B, I – B and J – B. Subsequently, the combination differences of the C levels and their energies as resulting from the analysis of the systems GK – C, H – C, I – C, and J – C were added. New energies allowed us to expand the analysis ro-vibrational levels towards higher N and v quantum numbers for $B^1\Sigma_u^+$, $C^1\Pi_u$, $EF^1\Sigma_g^+$, $GK^1\Sigma_g^+$, $H^1\Sigma_g^+$, $I^1\Pi_g$ and $J^1\Delta_g$. Finally, the precise determination of the

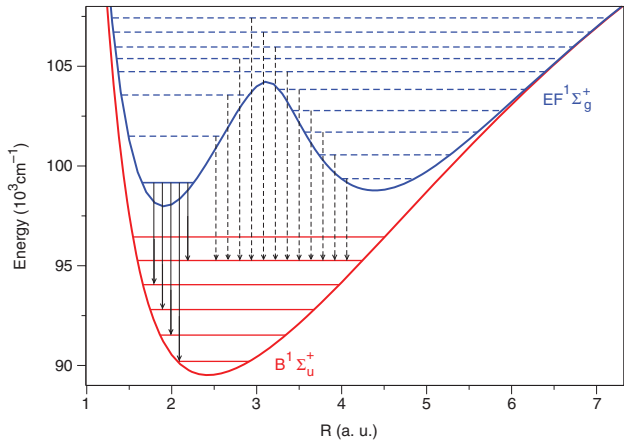

Figure 5. Schematic of the method by which the level energies are determined in the present study. Energy levels in $EF^1\Sigma_g^+$ and $B^1\Sigma_u^+$, and all other excited states are interconnected in the FT-spectra by a large number of spectral lines.

$EF^1\Sigma_u^+$ (v, N) allows us to carry out the analysis of the $B'^1\Sigma_u^+ - EF^1\Sigma_g^+$ and $D^1\Pi_u - EF^1\Sigma_g^+$ systems.

The spectral assignment was performed in a number of iterative steps. In view of the extreme density of lines in many cases a choice had to be made for the rovibronic assignment. Those were then first checked on internal consistency verifying combination differences between levels. In second round the resulting level energies were compared with levels and transitions as published from previous studies in the literature; if deviations were found larger than the expected uncertainties in those studies, a reanalysis was made sometimes leading to a reassignment. The vast amount of spectral lines in the FT-spectra usually permits alternative assignments. In this way the present study, which is more accurate than all previous ones, relies on the identifications in previous work.

Each combination difference or each level energy results from the subtraction or the addition of two line frequencies. These quantities were weighted with the weight $w=1/\gamma^2$ assigned to each line frequency, where γ is the FWHM linewidth. Furthermore, the signal to noise ratio (SNR) can be very different from one record to another, which introduces additional uncertainty in the determination of the transition frequency, and thereby of the level energies. Therefore, it has been necessary to take into account the SNR to refine the uncertainties in the level energies. In addition, we have included the uncertainties of the anchor lines: 0.00011 cm^{-1} for para-hydrogen and 0.00019 cm^{-1} for ortho-hydrogen. Consequently, a level energy bears an uncertainty, which depends on the number of lines and on uncertainties of the transition

frequencies used to calculate it. In this study we present excitation energies of some 547 levels in the singlet manifold of hydrogen, based on 4754 ro-vibronic assignments for over 25,200 spectral lines observed in 61 records of Fourier transform spectrograms. Thanks to the comprehensive analyses of the large number of records and ro-vibrational assignments, it has been possible to determine the level energies with extreme accuracy. This procedure of combining these uncertainties and averaging the obtained values from the large number of records, results in the uncertainties as stated in the tables below. Tables 2–10 report the final rovibronic energies of the electronic states $EF^1\Sigma_g^+$, $GK^1\Sigma_g^+$, $H^1\Sigma_g^+$, $B^1\Sigma_u^+$, $C^1\Pi_u$, $B'^1\Sigma_u^+$, $D^1\Pi_u$, $I^1\Pi_g$ and $J^1\Delta_g$ respectively.

The data in Tables 2–10 are extracted from a large database of transition frequencies of the Fourier transform emission study in many rovibronic bands. All these transition frequencies are made available electronically in the supplementary material to this paper on the *Mol. Phys.* website (H_2 rovibronic transitions 2000–22,000 cm^{-1}).

3. Results

In the following subsections the accurately determined level energies for the various states will be presented, discussed, and compared with previous determinations. In particular for the levels in the *gerade* manifolds the assignments of levels has some ambiguity as a result of strong mutual interactions, which were analysed by Yu and Dressler [19] and by Ross and Jungen [20]. Tsukiyama and co-workers studied these levels and provided alternative assignments in some cases [38–40]. Since the states are strongly mixed in some cases a definite assignment is difficult to make. Here we choose the most natural assignment from the experimentalists' perspective, that is by following the rotational ladder through the avoided crossings. This choice results in some assignments to be different from that of Ross and Jungen [20] who based the assignments on the wave function composition. For clarity, we present the ordering and assignment of levels in graphical form in Figure 6 for levels of $^1\Sigma_g^+$ and $^1\Pi_g$ symmetry, with only for the (+) or (e) parity component for the latter symmetry; for the (−) or (f) parity components no such ambiguities exist. In the subsections, each devoted to one electronic state investigated, we will briefly mention, in addition to the experimental determinations of level energies in previous studies, some results of *ab initio* and of multi-channel quantum defect calculations. The theoretical predictions of the level energies, from both approaches, are typically at an accuracy of $\sim 1\,cm^{-1}$. Hence, even the older experimental data were more accurate than theory, and the present improvements on the experimental side will not in each case be compared with the theoretical results.

3.1. *The* $EF^1\Sigma_g^+$ *state*

The first excited singlet gerade $EF^1\Sigma_g^+$ state in H_2 has been investigated thoroughly, starting with the classical work of Dieke on the $EF^1\Sigma_g^+ - B^1\Sigma_u^+$ system [9]. Davidson was the first to propose that the two bound E and F states in H_2 be described by a single adiabatic potential, connected by an avoided crossing at the intersection of the 1s2s Rydberg potential, forming the E state minimum, and the potential of the doubly excited ($2p\sigma^2$) state, giving rise to the F state minimum [41]. Early *ab initio* calculations were then performed by Gerhause and Taylor [42], and subsequently in the advanced framework with two-centered wave functions by Kolos and Wolniewicz [43]. The phenomenon of the double-well structure of the EF state and associated tunneling and predissociation phenomena were further investigated by Dressler and Wolniewicz with co-workers by means of *ab initio* calculations of increasing complexity [44–46]. The calculations were then compared with spectral assignments of levels in the inner and outer wells [47,48]. This work culminated in a final listing of level energies of the $EF^1\Sigma_g^+$ state and other states of *gerade* symmetry in the paper by Yu and Dressler [19]; a comparison of state-of-the-art *ab initio* calculations, which was the focus of their study, is made with classically obtained line positions. The alternative approach of MQDT has led to equally accurate calculation of level energies for the $EF^1\Sigma_g^+$ state [20].

Two-photon laser excitation of the $EF^1\Sigma_g^+$ state in H_2 was first demonstrated by Kligler and Rhodes, who monitored fluorescence in the visible domain [49]. Zare and co-workers thereafter showed that $2+1$ resonance-enhanced multi-photon ionisation (REMPI) can probe both inner and outer well states [50]. Precision studies to bridge the EF – X interval were performed by Glab and Hessler [51], and in a number of subsequent studies by Eyler and co-workers [52–55]. An order of magnitude improvement in accuracy was obtained in the study by Hannemann *et al.* achieving an accuracy of $\Delta\lambda/\lambda$ of 1×10^{-9}. Calibrated frequencies of the Q(0) to Q(2) lines in the $EF^1\Sigma_g^+ - X^1\Sigma_g^+$ (0,0) band were presented in [29], while additional Q(3) to Q(5) lines were used in [28]. The values of these transition energies are listed in Table 1.

Table 2. Level energies (term values) in the $EF^1\Sigma_g^+$ states of H_2 for vibrational levels $v=0$–28. The vibrational assignment is given in terms of a combined numbering in the double-well potential as well as separately for the E and F wells. This vibrational progression follows our 'natural assignment' as represented in Figure 6. The level energy for EF ($v=4$, $N=5$) marked with (*) is tentative (see text). Values are in cm^{-1} with the uncertainties in brackets ( ) relate to units of the last digits of the upright term values, not including any extra digits given as subscripts, and specify 1σ uncertainties.

N	EF ($v=0$) *E0*		EF ($v=1$) *F0*		EF ($v=2$) *F1*		EF ($v=3$) *E1*	
0	99164.78702	(15)	99363.8875 $_{8}$	(4)	100558.851 $_{62}$	(1)	101494.74402	(15)
1	99228.21824	(19)	99376.0474 $_{2}$	(4)	100570.8430 $_{5}$	(3)	101554.0269 $_{7}$	(2)
2	99354.55632	(14)	99400.512 $_{24}$	(1)	100594.8070 $_{1}$	(6)	101671.64197	(15)
3	99542.7660 $_{7}$	(2)	99437.1665 $_{3}$	(5)	100630.7127 $_{2}$	(3)	101849.4044 $_{9}$	(2)
4	99791.32519	(15)	99485.971 $_{96}$	(3)	100678.510 $_{38}$	(1)	102081.0311 $_{5}$	(2)
5	100098.2609 $_{2}$	(2)	99546.868 $_{64}$	(1)	100738.1316 $_{6}$	(6)	102367.1451 $_{8}$	(2)
6	100461.1973 $_{3}$	(2)			100809.502 $_{52}$	(2)	102701.554 $_{92}$	(4)
7	100877.3708 $_{0}$	(2)			100892.549 $_{19}$	(1)		
8	101343.8245 $_{1}$	(3)						
9	101857.1748 $_{2}$	(2)						
10	102414.0458 $_{8}$	(5)						
11	103010.4999 $_{3}$	(3)						
12	103641.5428 $_{6}$	(8)						
13	104303.018 $_{34}$	(4)						

N	EF ($v=4$) *F2*		EF ($v=5$) *F3*		EF ($v=6$) *E2*		EF ($v=7$) *F4*	
0	101698.951 $_{96}$	(2)	102778.228 $_{25}$	(1)	103559.59794	(15)	103838.5656 $_{5}$	(4)
1	101710.8478 $_{3}$	(4)	102790.1364 $_{6}$	(3)	103605.6119 $_{8}$	(2)	103857.8468 $_{1}$	(2)
2	101735.0306 $_{2}$	(4)	102813.8838 $_{7}$	(4)	103690.14695	(14)	103902.9828 $_{8}$	(3)
3	101768.5780 $_{9}$	(3)	102849.3611 $_{7}$	(3)	103995.2119 $_{0}$	(2)	103789.9773 $_{1}$	(2)
4	101816.1295 $_{7}$	(9)	102896.461 $_{94}$	(1)	104159.80598	(15)	103876.3768 $_{5}$	(3)
5	101874.8505 $_{1}$ *	(5)	102955.1176 $_{7}$	(7)	104386.8711 $_{4}$	(2)	103953.0198 $_{1}$	(4)
6	101945.009 $_{9}$	(4)	103025.519 $_{04}$	(2)			104396.442 $_{05}$	(2)
7	102026.5741 $_{0}$	(6)	103106.663 $_{20}$	(3)			104989.956 $_{05}$	(5)
8			103199.241 $_{86}$	(4)			103838.5656 $_{5}$	(4)

N	EF ($v=8$) *F5*		EF ($v=9$) *E3*		EF ($v=10$)		EF ($v=11$)	
0	104730.5923 $_{1}$	(8)	105384.9129 $_{0}$	(2)	105966.1527 $_{1}$	(8)	106713.0458 $_{9}$	(5)
1	104747.3423 $_{1}$	(3)	105415.2551 $_{9}$	(2)	105991.2171 $_{5}$	(2)	106734.2282 $_{3}$	(3)
2	104780.218 $_{90}$	(4)	105473.96704	(15)	106042.5481 $_{2}$	(4)	106776.4459 $_{8}$	(4)
3	104828.3982 $_{5}$	(3)	105556.8403 $_{3}$	(2)	106122.3648 $_{8}$	(3)	106839.6678 $_{0}$	(3)
4	104891.6909 $_{2}$	(9)	105657.7072 $_{0}$	(3)	106232.9271 $_{1}$	(4)	106924.5280 $_{9}$	(6)
5	104972.0087 $_{1}$	(3)	105770.1314 $_{4}$	(3)	106374.1301 $_{3}$	(3)	107033.0022 $_{1}$	(6)

N	EF ($v=12$)		EF ($v=13$)		EF ($v=14$)		EF ($v=15$)	
0	107425.8433 $_{8}$	(6)	108098.4828 $_{6}$	(5)	108793.5127 $_{2}$	(8)	109493.862 $_{22}$	(2)
1	107449.6180 $_{5}$	(2)	108122.1662 $_{1}$	(3)	108814.7762 $_{0}$	(3)	109514.6472 $_{5}$	(4)
2	107496.5311 $_{8}$	(3)	108169.5762 $_{6}$	(3)	108857.3759 $_{3}$	(4)	109555.8956 $_{6}$	(7)
3	107565.3271 $_{8}$	(3)	108240.6288 $_{0}$	(3)	108921.5417 $_{6}$	(3)	109617.0661 $_{8}$	(5)
4	107654.281 $_{33}$	(1)	108334.7489 $_{9}$	(7)	109007.7279 $_{7}$	(8)	109697.637 $_{75}$	(2)
5	107761.6899 $_{2}$	(7)	108450.405 $_{00}$	(3)	109116.5370 $_{8}$	(5)	109797.451 $_{10}$	(4)

N	EF ($v=16$)		EF ($v=17$)		EF ($v=18$)		EF ($v=19$)	
0	110163.3433 $_{3}$	(9)	110794.156 $_{94}$	(1)	111370.657 $_{80}$	(1)	112106.044 $_{16}$	(5)
1	110185.0710 $_{7}$	(4)	110815.1784 $_{2}$	(4)	111387.144 $_{27}$	(1)	112126.1482 $_{0}$	(6)
2	110228.1677 $_{8}$	(7)	110857.5131 $_{4}$	(7)	111420.668 $_{8}$	(4)	112167.804 $_{92}$	(1)
3	110291.8400 $_{0}$	(3)	110921.5971 $_{3}$	(4)	111472.533 $_{8}$	(1)	112230.8714 $_{2}$	(9)
4	110374.764 $_{47}$	(1)	111007.608 $_{67}$	(2)	111544.971 $_{95}$	(9)	112315.879 $_{58}$	(1)
5	110475.207 $_{07}$	(1)	111114.581 $_{18}$	(1)	111641.800 $_{9}$	(2)	112421.403 $_{96}$	(3)

(*continued*)

Table 2. Continued.

N	EF ($v=20$)		EF ($v=21$)		EF ($v=22$)		EF ($v=23$)	
0	112711.783 $_{5}$	(5)	113258.183 $_{5}$	(7)	113861.3805	(4)	114510.48 $_{85}$	(1)
1	112729.053 $_{0}$	(1)	113277.710 $_{6}$	(1)	113879.358 $_{7}$	(2)	114528.546 $_{6}$	(3)
2	112763.909 $_{5}$	(2)	113316.620 $_{6}$	(3)	113920.241 $_{0}$	(6)	114566.185 $_{3}$	(9)
3	112818.800 $_{2}$	(1)	113378.422 $_{2}$	(4)	113987.540 $_{8}$	(2)	114636.149 $_{1}$	(3)
4	112887.012 $_{5}$	(3)	113434.292 $_{5}$	(8)	114075.259 $_{1}$	(8)	114620.095 $_{9}$	(4)
5	112966.327 $_{2}$	(4)	113536.168 $_{0}$	(4)	114173.45 $_{62}$	(2)	114711.60 $_{66}$	(1)
N	EF ($v=24$)		EF ($v=25$)		EF ($v=26$)		EF ($v=27$)	
0	115024.789 $_{8}$	(4)	115563.75 $_{76}$	(1)			116508.080 $_{5}$	(5)
1	115043.907 $_{5}$	(8)	115577.717 $_{7}$	(3)	116031.668 $_{6}$	(3)	116523.527 $_{8}$	(3)
2	115079.889 $_{6}$	(8)	115606.692 $_{9}$	(9)	116047.290 $_{3}$	(9)	116554.487 $_{1}$	(9)
3	115131.078 $_{6}$	(2)	115653.885 $_{9}$	(4)	116088.621 $_{9}$	(4)	116604.092 $_{2}$	(4)
4	115207.286 $_{8}$	(7)	115692.83 $_{88}$	(2)	116151.563 $_{3}$	(6)	116633.396 $_{4}$	(8)
5	115275.732 $_{1}$	(8)	115777.601 $_{9}$	(4)	116232.397 $_{1}$	(7)	116722.051 $_{6}$	(8)
N	EF ($v=28$)							
0	116915.37 $_{73}$	(1)						
1	116931.887 $_{7}$	(4)						
2	116964.345 $_{8}$	(4)						
3	117016.209 $_{5}$	(5)						

Additional two-colour two-photon laser studies were performed on a number of higher vibrational levels in the $EF^1\Sigma_g^+$ state. Tsukiyama and co-workers probed the vibrational levels $v=19$–21 [38], and subsequently the levels $v=31$–32 [39] and $v=24$–29 [40]. In a similar scheme Ubachs and co-workers remeasured the $v=31$–32 levels [56], and with higher resolution for the $v=19$ level in the $EF^1\Sigma_g^+$ state [57].

In the present FT study, level energies in the $EF^1\Sigma_g^+$ state are determined for vibrational levels $v=0$–28. The $EF^1\Sigma_g^+ - B^1\Sigma_u^+$ system is by far the strongest system observed, yielding also the most extensive and most accurate information. Further EF-levels are observed in $EF^1\Sigma_g^+ - C^1\Pi_u$, $D^1\Pi_u - EF^1\Sigma_g^+$, and $B'^1\Sigma_u^+ - EF^1\Sigma_g^+$ systems. In Table 2 the results for the deduced level energies are presented. For EF, $v=0$ level energies of the lowest 14 rotational states are determined, while for subsequent vibrational states more limited numbers of rotational states are found in the spectra. Uncertainties are derived from a statistical analysis of all the line positions involving the specific level; the resulting uncertainties are placed in brackets in Table 2. Based on these estimates the level energies are generally better than $0.001\,cm^{-1}$ for lower vibrational (and rotational) quantum numbers up to $v=19$. For the higher vibrational levels ($v>19$), the uncertainty is still better than $0.01\,cm^{-1}$.

First we make a comparison with the comprehensive data set of Yu and Dressler [19]. For the levels $v=0$–11, the data are consistent with each other with an rms standard deviation of $0.02\,cm^{-1}$. For the vibrational levels $v>12$ there is a systematic shift, with the present data at lower energy at some $0.02\,cm^{-1}$ at $v=12$, at $0.04\,cm^{-1}$ at $v=16$ and higher. Hence for the entire EF (v,N) manifold we find agreement with Yu and Dressler [19] within a few $0.01\,cm^{-1}$, which may be considered good. However, there is one specific level, EF ($v=4$, $N=5$), where we determine a level energy (at $101874.8505\,cm^{-1}$) that deviates by $0.2\,cm^{-1}$ from the previously determined value, thus clearly outside the error limits. In the FT-spectra we find a level (at $101875.05\,cm^{-1}$) that might be an alternate assignment, but we keep the listed value, however as tentative; this is an exceptional case where the previously determined values do not provide guidance in the assignment. For some higher lying levels in EF $v=24$–28, a few level energies have deviations of 0.10–$0.15\,cm^{-1}$. In view of the fact that transitions involving these levels are much weaker than the lower lying ones (not only in the present studies, but also in previous studies), we regard these deviations as reasonable.

We note that the values contained in [19] rely on the lowest EF-levels of Jungen *et al.* [31]. Jungen *et al.* also report on FT-spectra on transitions between excited states of the H_2 molecule, and the determination of the level energies of the excited states is similar to our procedure based on *anchor lines* that are also adopted

Table 3. Level energies in the GK $^1\Sigma_g^+$ state of H_2 for vibrational levels $v=0$–6. Values in cm^{-1}.

N	GK ($v=0$)		GK ($v=1$)		GK ($v=2$)		GK ($v=3$)	
0	111628.811$_1$	(5)	111812.629$_{01}$	(4)	113393.440$_2$	(6)	114044.568$_3$	(8)
1	111650.285$_5$	(1)	111805.110$_{14}$	(1)	113418.857$_0$	(2)	114030.871$_4$	(2)
2	111693.728$_4$	(1)	111827.733$_{83}$	(1)	113470.560$_3$	(3)	114046.342$_7$	(3)
3	111759.941$_1$	(1)	111893.0788$_4$	(8)	113550.359$_0$	(2)	114093.595$_8$	(1)
4	111845.249$_6$	(3)	112005.477$_{37}$	(2)	113662.426$_8$	(4)	114180.217$_5$	(2)
5	111941.701$_3$	(4)	112169.981$_{28}$	(1)	113772.464$_2$	(3)	114318.559$_6$	(1)
6	112052.45$_{87}$	(2)	112387.425$_{79}$	(3)			114508.071$_9$	(6)
7			112640.877$_{64}$	(4)			114744.939$_0$	(2)
8			112986.494$_{34}$	(7)			115035.519$_7$	(5)
9			113349.35$_{043}$	(1)			115391.19$_{35}$	(1)

N	GK ($v=4$)		GK ($v=5$)		GK ($v=6$) *W2*	
0	115099.829$_3$	(8)	116164.637$_3$	(8)	117081.398$_2$	(2)
1	115136.740$_{96}$	(1)	116233.784$_3$	(4)	117106.473$_6$	(1)
2	115207.323$_{69}$	(1)	116349.110$_1$	(2)	117156.368$_0$	(2)
3	115310.0163$_5$	(1)	116495.004$_5$	(1)	117232.048$_1$	(2)
4	115450.269$_{05}$	(1)	116701.857$_3$	(7)	117340.448$_5$	(3)
5	115646.201$_{92}$	(2)	116883.505$_4$	(3)	117520.535$_4$	(4)

from the lowest EF, $v=0$ levels. However, the anchor lines in [31] are the old and less accurate values of [52]. Comparison with the present two-photon data on the EF-calibrations [28,29] shows that the level energies of Jungen *et al.* [31], and therewith also the level energies of Yu and Dressler [19] are too high by $0.014\,cm^{-1}$. For most part, this explains the offset between the present and previous FTIR data sets.

In the present listing in Table 2 we have chosen assignments for the EF $^1\Sigma_g^+$ state that differ from those of Ross and Jungen [20], with our assignments graphically illustrated in Figure 6. Yu and Dressler in the text of the paper and in particular in Table V of [19] use assignments in terms of Y1 (corresponding to EF21), Z1 (EF22), U1 (EF23), X1 (EF25), Z2 (EF26) and Y2 (EF28), which relate to the original assignments used in the Dieke atlas. The labels inside the parentheses indicate the EF assignments, which were used in the PAPS deposit associated with Ref. [19]. Here we adopt this assignment in terms of EF states.

In comparison with the data of Tsukiyama and co-workers [38], remarkable agreement is found within $0.01\,cm^{-1}$ for all EF($v=19$) levels. Similarly for EF($v=20$) agreement is found within a few $0.01\,cm^{-1}$, except for N=4, which is off by $0.6\,cm^{-1}$ with respect to both the present data and those of [19], which leads us to conclude an error in [38]. For EF($v=21$) again good agreement is found, where we have a different assignment for the $N=4$ level following Figure 6. The data on EF($v=24$) up to EF($v=28$) [40] are found to be in agreement with the present findings, where the laser data are systematically shifted upward by some $0.05\,cm^{-1}$, which is reasonable for a pulsed laser experiment based on commercial dye lasers.

The data of de Lange *et al.* [57] on EF ($v=19$) allow for an accurate comparison with our data, and therewith a verification, since their values are accurate within $0.006\,cm^{-1}$ (1σ). Four of the five levels observed (for $N=1$–5) fall within the 1σ uncertainty, while on average the data of [57] are shifted by $-0.004\,cm^{-1}$. We regard this as a convincing consistency check on both data sets, which have comparable accuracies for EF ($v=19$).

3.2. *The* GK $^1\Sigma_g^+$ *state*

The GK $^1\Sigma_g^+$ state is the second double well state of $^1\Sigma_g^+$ symmetry. It has been treated in the early *ab initio* calculations by Dressler, Wolniewicz and co-workers [44,58]. Later, after improved calculations [19] the first 9 vibrational levels pertaining to this potential have been assigned. Strong interactions between the various states of $^1\Sigma_g^+$ and $^1\Pi_g$ symmetry hamper an unambiguous identification; again in the text and tables of [19] some levels are assigned by 'W' and 'X', dating back to the assignments of Dieke. We take the W2 level as GK($v=6$). For the assignment of lines of GK(5), we follow the assignment of Ross and Jungen [20] and of Ishii *et al.* [40], which is different from that of Yu and

Table 4. Level energies in the $H^1\Sigma_g^+$ state of H_2 for vibrational levels $v=0$–2. Values in cm^{-1}.

N	H ($v=0$)		H ($v=1$)		H ($v=2$)	
0	112957.559 $_{84}$	(1)	115251.502 $_{4}$	(5)	117297.069 $_{3}$	(7)
1	113016.7423 $_{4}$	(6)	115296.922 $_{3}$	(1)	117338.524 $_{4}$	(4)
2	113134.067 $_{91}$	(2)	115393.820 $_{6}$	(3)	117455.509 $_{8}$	(2)
3	113303.4403 $_{4}$	(8)	115544.946 $_{1}$	(4)	117590.233 $_{3}$	(3)
4	113548.795 $_{36}$	(3)			117759.242 $_{5}$	(8)
5	113860.362 $_{88}$	(6)			117999.511 $_{2}$	(4)

Table 5. Level energies in the $B^1\Sigma_u^+$ state of H_2 for vibrational levels $v=0$–13. Values in cm^{-1}.

N	B ($v=0$)		B ($v=1$)		B ($v=2$)		B ($v=3$)	
0	90203.49985	(11)	91521.82475	(15)	92803.3007 $_{9}$	(2)	94050.0108 $_{6}$	(3)
1	90242.3381 $_{1}$	(2)	91558.7249 $_{4}$	(3)	92838.5583 $_{9}$	(3)	94083.8145 $_{9}$	(3)
2	90319.64269	(14)	91632.2020 $_{1}$	(3)	92908.78707	(15)	94151.16500	(15)
3	90434.6796 $_{5}$	(2)	91741.6225 $_{0}$	(5)	93013.4211 $_{1}$	(3)	94251.5492 $_{4}$	(3)
4	90586.3775 $_{0}$	(3)	91886.0530 $_{8}$	(2)	93151.62962	(15)	94384.2121 $_{6}$	(2)
5	90773.3593 $_{5}$	(5)	92064.2938 $_{2}$	(5)	93322.3367 $_{2}$	(3)	94548.1738 $_{1}$	(5)
6	90993.9775 $_{9}$	(3)	92274.9023 $_{1}$	(3)	93524.2452 $_{9}$	(3)	94742.2539 $_{2}$	(4)
7	91246.3738 $_{7}$	(4)	92516.2362 $_{0}$	(5)	93755.8737 $_{9}$	(7)	94965.091 $_{84}$	(4)
8	91528.5155 $_{3}$	(2)	92786.4891 $_{1}$	(5)	94015.5785 $_{3}$	(3)	95215.165 $_{00}$	(3)
9	91838.2518 $_{0}$	(8)	93083.7343 $_{3}$	(6)	94301.5980 $_{7}$	(7)	95490.8480 $_{2}$	(7)
10	92173.3753 $_{0}$	(3)	93405.9694 $_{4}$	(3)	94612.0897 $_{8}$	(5)		
11	92531.6503 $_{0}$	(2)	93751.1504 $_{4}$	(7)	94945.1527 $_{7}$	(1)		
12	92910.8984 $_{3}$	(9)	94117.231 $_{05}$	(2)	95298.8812 $_{8}$	(7)		
13					95671.370 $_{50}$	(2)		
N	B ($v=4$)		B ($v=5$)		B ($v=6$)		B ($v=7$)	
0	95263.0277 $_{0}$	(4)	96443.0271 $_{2}$	(3)	97590.5317 $_{2}$	(5)	98706.0107 $_{7}$	(5)
1	95295.5100 $_{8}$	(3)	96474.2818 $_{0}$	(2)	97620.6205 $_{4}$	(6)	98734.9180 $_{0}$	(4)
2	95360.23720	(15)	96536.5721 $_{7}$	(2)	97680.6069 $_{1}$	(2)	98792.61094	(15)
3	95456.7430 $_{7}$	(3)	96629.4727 $_{4}$	(3)	97770.0977 $_{6}$	(4)	98878.7888 $_{3}$	(4)
4	95584.3352 $_{5}$	(2)	96752.3439 $_{7}$	(2)	97888.5137 $_{5}$	(3)	98992.9382 $_{1}$	(3)
5	95742.1146 $_{5}$	(6)	96904.3557 $_{8}$	(4)	98035.0798 $_{7}$	(7)	99134.344 $_{33}$	(1)
6	95928.9842 $_{9}$	(4)	97084.4918 $_{3}$	(4)	98208.974 $_{98}$	(2)	99302.100 $_{60}$	(1)
7	96143.695 $_{54}$	(4)			98408.623 $_{20}$	(2)		
N	B ($v=8$)		B ($v=9$)		B ($v=10$)		B ($v=11$)	
0	99789.9191 $_{7}$	(4)	100842.7319 $_{8}$	(3)	101864.9344 $_{9}$	(5)	102857.0266 $_{6}$	(6)
1	99817.9578 $_{8}$	(4)	100869.6120 $_{0}$	(5)	101891.2328 $_{3}$	(7)	102882.1159 $_{9}$	(8)
2	99873.8857 $_{4}$	(2)	100923.2800 $_{9}$	(1)	101943.7821 $_{4}$	(3)	102932.2179 $_{1}$	(2)
3	99957.4178 $_{4}$	(4)	101003.5037 $_{6}$	(4)	102022.6417 $_{4}$	(5)	103007.13912	(19)
4	100068.2015 $_{3}$	(4)	101109.8691 $_{4}$	(2)	102129.2272 $_{9}$	(5)	103106.5349 $_{9}$	(3)
5	100206.185 $_{42}$	(2)	101241.7707 $_{8}$	(4)			103229.913 $_{67}$	(2)
N	B ($v=12$)		B ($v=13$)					
0	103819.5225 $_{0}$	(6)	104752.940 $_{05}$	(1)				
1	103844.5343 $_{0}$	(9)	104776.414 $_{29}$	(1)				
2	103895.1340 $_{4}$	(3)	104823.3190 $_{2}$	(5)				
3	103976.408 $_{30}$	(3)	104893.469 $_{76}$	(2)				
4	104045.7890 $_{8}$	(4)	104986.6099 $_{0}$	(7)				
5	104172.590 $_{17}$	(1)	105102.401 $_{60}$	(6)				

Table 6. Level energies in the $C^1\Pi_u$ state of H_2 for vibrational levels $v=0$–3. Values in cm^{-1}.

N	C^+ ($v=0$)		C^- ($v=0$)		C^+ ($v=1$)		C^- ($v=1$)	
1	99152.059 $_{51}$	(2)	99150.8516 $_{5}$	(5)	101457.5690 $_{1}$	(9)	101456.3442 $_{7}$	(8)
2	99275.8297 $_{7}$	(4)	99272.3582 $_{5}$	(7)	101574.9639 $_{3}$	(4)	101571.5631 $_{2}$	(9)
3	99459.9488 $_{4}$	(4)	99453.4335 $_{2}$	(5)	101749.1534 $_{5}$	(6)	101743.2410 $_{6}$	(1)
4	99702.6511 $_{8}$	(5)	99692.669 $_{89}$	(3)	101976.605 $_{15}$	(7)	101970.043 $_{12}$	(3)
5	100001.144 $_{3}$	(3)	99988.281 $_{02}$	(3)	102294.170 $_{63}$	(4)	102250.235 $_{00}$	(2)
6			100338.044 $_{24}$	(7)	102610.526 $_{40}$	(5)	102581.606 $_{70}$	(4)
7							102962.145 $_{12}$	(4)
N	C^+ ($v=2$)		C^- ($v=2$)		C^+ ($v=3$)		C^- ($v=3$)	
1	103628.665 $_{09}$	(6)	103627.8560 $_{9}$	(7)	105660.713 $_{1}$	(3)	105668.0822 $_{0}$	(3)
2	103738.4627 $_{7}$	(7)	103736.940 $_{17}$	(3)	105783.757 $_{3}$	(1)	105771.126 $_{90}$	(2)
3	103895.959 $_{22}$	(2)	103899.441 $_{50}$	(1)	105938.546 $_{2}$	(5)	105924.621 $_{20}$	(2)
4	104141.627 $_{07}$	(3)	104114.096 $_{25}$	(2)	106144.062 $_{6}$	(3)	106127.311 $_{60}$	(7)
5	104403.464 $_{40}$	(8)	104379.225 $_{35}$	(2)	106397.043 $_{8}$	(8)		
6	104718.714 $_{29}$	(6)	104692.909 $_{63}$	(3)				
7			105052.72 $_{930}$	(1)				

Table 7. Level energies in the $B'^1\Sigma_u^+$ state of H_2 for vibrational levels $v=0$–3. Values in cm^{-1}.

N	B′ ($v=0$)		B′ ($v=1$)		B′ ($v=2$)		B′ ($v=3$)	
0	110478.5399 $_{9}$	(3)	112358.5811 $_{9}$	(3)	114075.2169 $_{8}$	(2)	115606.4790 $_{8}$	(4)
1	110529.4148 $_{4}$	(7)	112404.4426 $_{9}$	(3)	114118.3519 $_{6}$	(2)	115647.0450 $_{3}$	(4)
2	110630.8213 $_{3}$	(2)	112496.1851 $_{9}$	(15)	114204.4154 $_{0}$	(1)	115728.0738 $_{8}$	(1)
3	110782.0710 $_{7}$	(3)	112633.6854 $_{5}$	(3)	114332.9670 $_{1}$	(6)	115849.4711 $_{8}$	(5)
4	110982.1341 $_{5}$	(2)	112816.4707 $_{9}$	(15)	114503.2778 $_{4}$	(2)	116011.5202 $_{7}$	(5)
5	111229.6470 $_{9}$	(9)	113043.599 $_{92}$	(1)	114714.299 $_{60}$	(1)		
6	111522.8962 $_{7}$	(5)			114964.623 $_{20}$	(2)		
7	111859.892 $_{64}$	(1)						

Table 8. Level energies in the $D^1\Pi_u$ state of H_2 for vibrational levels $v=0$–2. Values in cm^{-1}.

N	D^+ ($v=0$)		D^- ($v=0$)		D^+ ($v=1$)		D^- ($v=1$)		D^+ ($v=2$)		D^- ($v=2$)	
1	112935.281 $_{31}$	(5)	112931.659 $_{86}$	(1)	115155.804 $_{8}$	(4)	115154.407 $_{5}$	(6)	117251.705 $_{9}$	(4)	117247.8630 $_{9}$	(6)
2	113059.7180 $_{7}$	(5)	113049.293 $_{62}$	(4)	115269.651 $_{91}$	(1)	115265.911 $_{1}$	(6)	117363.322 $_{7}$	(2)	117353.380 $_{64}$	(5)
3	113244.077 $_{40}$	(3)	113224.6070 $_{7}$	(3)	115437.952 $_{7}$	(2)	115431.971 $_{6}$	(6)	117526.890 $_{5}$	(1)	117510.5466 $_{8}$	(5)
4	113486.041 $_{66}$	(4)	113456.222 $_{23}$	(4)	115657.511 $_{5}$	(2)	115651.412 $_{5}$	(9)	117738.446 $_{5}$	(3)	117718.179 $_{67}$	(3)
5			113742.355 $_{37}$	(3)			115922.53 $_{29}$	(1)			117974.570 $_{58}$	(2)
6			114080.951 $_{09}$	(6)								
7			114469.484 $_{99}$	(3)								

Dressler [19]. For the ambiguous assignments we refer to Figure 6, where we have indicated the rotational progressions of the $^1\Sigma_g^+$ and $^1\Pi_g^+$ levels that have led us to the chosen identification. In the present FT-emission study we have observed up to $GK^1\Sigma_g^+$ ($v=6$), for which the data are listed in Table 3.

Comparing the present results with those of [19] we find agreement within $0.02\,cm^{-1}$ for the lowest vibrational levels up to GK($v=4$). The GK($v=3$) level for $N=0$ is lower by $0.09\,cm^{-1}$ with respect to [19].

Tsukiyama *et al.* using double-resonance laser excitation observed $GK^1\Sigma_g^+$, $v=0$–2 [38]. All 15 lines are within $0.06\,cm^{-1}$, while most agree within $0.02\,cm^{-1}$. De Lange *et al.* [57] observed $GK^1\Sigma_g^+$, $v=0$ at higher precision ($0.006\,cm^{-1}$). The two levels, $N=2$ and $N=3$ are higher in energy with respect to De

Table 9. Level energies in the $I^1\Pi_g$ state of H_2 for vibrational levels $v=0$–3. Values in cm^{-1}.

N	I^+ ($v=0$)		I^- ($v=0$)		I^+ ($v=1$)		I^- ($v=1$)	
1	112135.236 $_{91}$	(2)	112072.863 $_{98}$	(1)	114223.9470 $_{0}$	(4)	114172.095 $_{22}$	(1)
2	112282.267 $_{40}$	(3)	112147.626 $_{83}$	(1)	114353.725 $_{86}$	(1)	114252.8794 $_{7}$	(7)
3	112471.0364 $_{5}$	(9)	112272.0685 $_{2}$	(9)	114502.4711 $_{4}$	(6)	114379.092 $_{86}$	(2)
4	112703.686 $_{23}$	(3)	112449.0935 $_{4}$	(8)	114785.379 $_{40}$	(8)	114552.919 $_{65}$	(1)
5	–		112679.057 $_{91}$	(2)	115004.829 $_{20}$	(3)	114775.079 $_{70}$	(4)
6	113291.620 $_{88}$	(3)	112961.096 $_{58}$	(3)			115045.125 $_{69}$	(2)
7	113701.409 $_{40}$	(8)	113293.457 $_{38}$	(9)				
8			113674.027 $_{40}$	(9)				
9			114101.489 $_{70}$	(3)				
10			114569.16 $_{500}$	(1)				

N	I^+ ($v=2$)		I^- ($v=2$)		I^+ ($v=3$)		I^- ($v=3$)	
1	116103.609 $_{9}$	(2)	116114.3010 $_{6}$	(9)	117940.136 $_{2}$	(1)	117881.460 $_{4}$	(3)
2	116148.288 $_{2}$	(2)	116197.5009 $_{7}$	(8)	118027.201 $_{6}$	(5)	117964.098 $_{2}$	(1)
3	116214.186 $_{0}$	(3)	116323.956 $_{59}$	(2)	118139.270 $_{7}$	(3)	118088.261 $_{3}$	(3)
4	116305.278 $_{2}$	(4)	116494.578 $_{99}$	(2)	118257.59 $_{92}$	(1)	118253.948 $_{4}$	(4)
5	116424.434 $_{8}$	(6)	116709.641 $_{07}$	(4)			118460.839 $_{6}$	(8)
6	116573.342 $_{2}$	(8)	116968.697 $_{40}$	(5)				

Table 10. Level energies in the $J^1\Delta_g$ state of H_2 for vibrational levels $v=0$–2. Values in cm^{-1}.

N	J^+ ($v=0$)		J^- ($v=0$)		J^+ ($v=1$)		J^- ($v=1$)		J^+ ($v=2$)		J^-($v=2$)	
2	112536.7484 $_{5}$	(5)	112525.955 $_{01}$	(1)	114721.398 $_{80}$	(2)	114718.212 $_{9}$	(2)	116787.679 $_{4}$	(2)	116787.229 $_{2}$	(5)
3	112774.584 $_{53}$	(1)	112743.5527 $_{0}$	(3)	114923.4519 $_{8}$	(2)	114914.494 $_{2}$	(3)	116960.087 $_{7}$	(2)	116963.152 $_{0}$	(3)
4	113078.128 $_{30}$	(8)	113018.3700 $_{1}$	(4)	115164.888 $_{50}$	(5)	115166.533 $_{8}$	(3)	117193.174 $_{8}$	(3)	117191.590 $_{9}$	(1)
5	113415.499 $_{90}$	(2)	113346.500 $_{66}$	(3)	115459.48 $_{950}$	(2)	115470.26 $_{73}$	(1)	117413.867 $_{0}$	(4)		
6			113724.735 $_{90}$	(7)								

Lange by 0.004 and 0.003 cm^{-1}, in good agreement and well within the 1σ boundaries.

3.3. *The* $H^1\Sigma_g^+$ *state*

The $H^1\Sigma_g^+$ state in H_2 is associated with the inner well of the third double well potential of $^1\Sigma_g^+$ symmetry. This structure has been treated in consecutive *ab initio* studies by Wolniewicz and Dressler [59–61]. After the first observation of the rovibrational levels pertaining to the outer well [62] further improved calculations were performed addressing adiabatic effects [63] and relativistic effects [64]. Finally a comparison between observed and most updated calculations was made in [65]. This work also led to accurate predictions for the $H^1\Sigma_g^+$ inner well states. Yu and Dressler [19] assigned the first three vibrational levels $v=0$–2, while in the work of Ross and Jungen the first two levels were calculated [20]. Tsukiyama *et al*. employed their double resonance technique to detect $H^1\Sigma_g^+$, $v=0$ [38].

In the present FT emission study we observed $H^1\Sigma_g^+$, $v=0$–2, with the values of the obtained level energies listed in Table 4. Comparison with [19] yields agreement within 0.01 cm^{-1} for levels up to $N=3$, with somewhat higher discrepancy for the higher rotational levels.

In a recent experiment involving lasers and mm-wave multiple-resonance schemes, the term value of the H, $v=0$, $N=3$ level was determined at 113303.463 (3) cm^{-1} [66]. The high accuracy achieved in this experiment presents us a means of verification of the states of *gerade* symmetry in the higher energy range. At first glance, a strong disagreement seems to persist with the present value. However, the reported value in [66] depends on a value of the ionisation potential of H_2, for which the authors adopted 124417.512 cm^{-1} [67]. Recently an accurate measurement was performed providing a highly accurate value for the ionisation potential of H_2, yielding 124417.49113 (37) cm^{-1} [68], which is consistent with

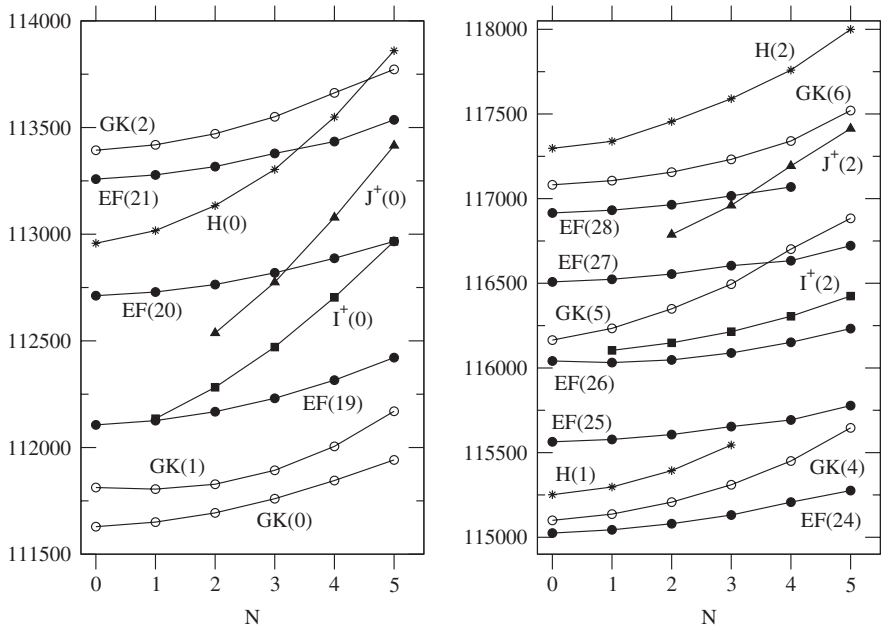

Figure 6. Graphical representation of the level energies of $^1\Sigma_g^+$ and $^1\Pi_g^+$ symmetries as a function of rotational quantum number N, in the energy range 111,500–114,000 cm^{-1} (left) and for the range 115,000–118,000 cm^{-1} (right). $EF^1\Sigma_g^+$ rovibrational levels are indicated by filled circles (•), $GK^1\Sigma_g^+$ levels as open circles (o), $H^1\Sigma_g^+$ levels as stars (*), $I^1\Pi_g^+$ levels as squares (■), and $^1\Delta_g^+$ levels as triangles (▲).

a more recent *ab initio* calculation [24]. This brings down the level energy of H, $v=0$, $N=3$ to 113303.442 (3) cm^{-1}, which is within the 1σ-boundaries with the present value of 113303.4403 (8) cm^{-1}. For comparison, Yu and Dressler report 113303.44 cm^{-1} [19] and Tsukiyama *et al.* report 113303.50 cm^{-1} [38], but the uncertainties in these studies are larger.

3.4. *The* $B^1\Sigma_u^+$ *state*

The $B^1\Sigma_u^+$ state, the lowest state of $^1\Sigma_u^+$ symmetry associated with a $2p\sigma_u$ orbital, is the upper state of the $B^1\Sigma_u^+ - X^1\Sigma_g^+$ Lyman band system, which has been investigated over the years, starting from the first observation by Lyman [7] after whom these bands have been named. Potential energy curves were calculated by *ab initio* methods by Kolos and Wolniewicz [69], improved by Wolniewicz and Dressler [70], with non-adiabatic corrections [71] and relativistic corrections [72] added later. Senn *et al.* [21] performed non-adiabatic coupling calculations to determine level energies, based on these potentials; in these calculations the couplings between the four lowest states of ungerade symmetry ($B^1\Sigma_u^+$, $C^1\Pi_u$, $B'^1\Sigma_u^+$, and $D^1\Pi_u$) were included. The same was done in the later coupled Schrödinger calculations by Abgrall *et al.* [25] but in the latter case the potential energy curves were adapted in a fitting procedure, to match the experimental data. Jungen and Atabek applied their MQDT formalism also to this lowest state of $^1\Sigma_u^+$ symmetry; although the $B^1\Sigma_u^+$ state is not of Rydberg character nevertheless good agreement was found with experiment [22].

Classical spectroscopy has resulted in the accurate studies by Dabrowski [11] and by the group at the Meudon Observatoire [13]. Both these studies resulted in an absolute accuracy of some 0.10 cm^{-1}. The use of lasers and harmonic generation to reach the XUV domain, has gradually improved the accuracy at which the $B^1\Sigma_u^+ - X^1\Sigma_g^+$ system was investigated. Early studies resulted in an accuracy of ~0.05 cm^{-1} [16,17] for the observed vibrational levels $v=10$–19. Later, with the use of more sophisticated pulsed dye amplification and calibration techniques, accuracies in the range 0.004–0.011 cm^{-1} were achieved. Philip *et al.* [18] covered the range of $B^1\Sigma_u^+$, $v=2$–18, while $B^1\Sigma_u^+$, $v=0$–2 were added [73], and the $B^1\Sigma_u^+$, $v=6$ was recalibrated [74] in separate studies. In the direct XUV-laser excitation studies accuracies of some 0.005 cm^{-1} or $\Delta\lambda/\lambda$ of 5×10^{-8} could be achieved. In the preliminary investigation on the combination scheme as depicted in Figure 5, it was demonstrated that level energies in the $B^1\Sigma_u^+$ state can be determined to an accuracy of some $\Delta\lambda/\lambda$ of 5×10^{-9} [28].

In the present FT emission study levels $B^1\Sigma_u^+$, $v = 0$–13 are observed, with many of the rovibrational lines at an accuracy of few 0.0001 cm^{-1}. The latter is due to the fact that B-levels are observed in a great number of vibrational bands including the strongest $EF^1\Sigma_g^+ - B^1\Sigma_u^+$ system, over which data is averaged. Although the values of Abgrall *et al.* [15] are less accurate, a comparison has been made. In particular, this is because the Abgrall *et al.* presents such a comprehensive data set that is often used in spectroscopic studies of H_2. In a comparison between the data of Table 5 and those of [15], we find that virtually all deviations are below 0.11 cm^{-1} with few exceptions. Overall, in the comparison between the Abgrall data set and the present values, there is an rms deviation of about 0.05 cm^{-1} and a systematic shift of 0.04 cm^{-1}. From this it may be concluded, that the classical data are rather accurate; if the systematic shift of 0.04 cm^{-1} is subtracted, then all levels may be considered to lie well within 0.1 cm^{-1} on an absolute energy scale.

A comparison with the direct XUV measurements is postponed to Section 3.10, where we discuss an updated derivation of Lyman transition wavelengths.

3.5. *The* $C^1\Pi_u$ *state*

The $C^1\Pi_u$ state, the lowest state of $^1\Pi_u$ symmetry in H_2 associated with a $2p\pi_u$-orbital, is the upper state of the $C^1\Pi_u - X^1\Sigma_g^+$ Werner band system, which was first observed by Werner in 1926 [75]. Early *ab initio* calculations for the $C^1\Pi_u$ state were performed by Kolos and Rychlewski [76], on which Jungen and Atabek [22] based their MQDT calculations for the $^1\Pi_u$ states. Later Wolniewicz and Staszewka obtained improved potential functions for the $^1\Pi_u$ states [77]. As for the $B^1\Sigma_u^+$ state, both Senn *et al.* [21] and Abgrall *et al.* [25] performed coupled channel equations to derive level energies.

The absorption spectrum of the Lyman and Werner systems are overlaid, so these systems are usually observed in the same spectroscopic studies. The important data are found in Dabrowski [11] and in the work of the Meudon group [13]. The laser based studies yield data on $C^1\Pi_u$, $v = 2$–5 [9] and $v = 0$–4 [18]. All rovibrational levels in a $^1\Pi_u$ state are split into two Λ-doublet components Π^+ and Π^-. (If excitation takes place in connection to $^1\Sigma_g^+$, the Π^+ component can be probed in P and R branches, while the Π^- component is probed in the Q branch.) The Π_u^+ components undergo strong interactions from nearby lying $^1\Sigma_u^+$ states; due to the accidental resonances in these perturbations [11,17] the energy shifts become somewhat erratic. In any case the Π_u^+ and Π_u^- components are treated as separate entities.

The present FT study yields information on level energies for both Π_u^+ and Π_u^- components of the $C^1\Pi_u$ state for vibrational levels $v = 0$–3, and the results are listed in Table 6. Since the spectral lines, from which line positions are determined (mainly $EF^1\Sigma_g^+ - C^1\Pi_u$), are weaker the accuracy is somewhat less than that for the $B^1\Sigma_u^+$ state. Nevertheless the accuracy is better than 0.001 cm^{-1} for $v = 0$ and a few times 0.001 cm^{-1} for the higher v-levels.

Similarly as for the $B^1\Sigma_u^+$ state a comparison can be made with the comprehensive data set of Abgrall *et al.* [15]. For the 46 level energies determined in the present study for $C^1\Pi_u$ ($v = 0$–3) we find that the data of [15] are shifted to higher energy by on average 0.07 cm^{-1}. If such an offset is taken into account most level energies agree to within a few 0.01 cm^{-1}, while there are no deviations larger than 0.15 cm^{-1}. In Section 3.10 a new line list of Werner line wavelengths are presented. In that section, an assessment based on the comparison with direct XUV measurements is also given.

3.6. *The* $B'^1\Sigma_u^+$ *state*

The $B'^1\Sigma_u^+$ state of H_2, is associated with a $3p\sigma_u$ orbital. Jungen and Atabek [22] had performed MQDT calculations on this state, deriving a potential energy curve, before this was obtained by *ab initio* methods by Kolos [78]. Again, as for the $B^1\Sigma_u^+$ and $C^1\Pi_u$ states, both Senn *et al.* [21] and Abgrall *et al.* [25] applied coupled Schrödinger equation calculations to derive level energies.

The $B'^1\Sigma_u^+ - X^1\Sigma_g^+$ band system was observed in a low-pressure emission discharge, revealing levels $v = 0$–7 at the typical accuracy of 0.10 cm^{-1} [25]. Previously Namioka had observed some of these bands at lower accuracy [79]. XUV laser methods were applied in the range 86–90 nm to calibrate a few transitions in the $B'^1\Sigma_u^+ - X^1\Sigma_g^+$ $(v, 0)$ bands for $v = 0$–2 [80].

In the present FT-emission study we have determined level energies for $B'^1\Sigma_u^+$, $v = 0$–2; results are listed in Table 7. A comparison was made with the comprehensive data set of [25], and we find that the presently determined values as listed in Table 7 are all within 0.1 cm^{-1} from those of [25]. An average shift is found in the classical data of only –0.025 cm^{-1}. The R(0) transitions of the XUV-laser study can be directly compared with the present level energies of $B'^1\Sigma_u^+$ ($N = 1$) level energies; deviations are found within 0.05 cm^{-1}, while the average shift is around 0.03 cm^{-1}. This can be considered as good agreement for pulsed laser excitation studies as those of [80].

3.7. *The* $D^1\Pi_u$ *state*

The $D^1\Pi_u$ state is associated with a $3p\pi_u$ orbital. Early *ab initio* calculation of its potential was performed by Kolos and Rychlewski [76], while improved potentials were obtained recently by Wolniewicz and Staszewska [77]. MQDT calculations are contained in the work of Jungen and Atabek [22], as for the other states of ungerade symmetry treated in the above.

Early observations were obtained by Namioka [79] and by Takezawa [81] in the $D^1\Pi_u - X^1\Sigma_g^+$ absorption system. From these studies it followed that the $D^1\Pi_u$ state is predissociated for vibrational levels $v>2$, for the $^1\Pi^+$ components. Experimental observation of improved accuracy of the $D^1\Pi_u - X^1\Sigma_g^+$ system was obtained in the study by Abgrall *et al.* [25], while a single vibrational level ($v=1$) was observed in XUV-laser excitation [80]. In the present FT-emission study level energies for both Π_u^+ and Π_u^- components for $D^1\Pi_u$, $v=0$–2 were determined, with the results listed in Table 8. The uncertainty is somewhat less than for the other systems and amounts to some $0.005\,cm^{-1}$. A comparison between the data of Table 8 and those of [25] yields good agreement, an rms deviation of some $0.06\,cm^{-1}$, without in this case a systematic shift. The present level energies are also in agreement within 1σ of the XUV-laser results [80]. We note a typographic error in the $D^1\Pi_u^-$, $v=2$, $N=5$ value of Abgrall *et al.* [25], which should read $117974.62\,cm^{-1}$ instead of $119974.62\,cm^{-1}$.

3.8. *The* $I^1\Pi_g$ *state*

The $I^1\Pi_g$ state, associated with a $3d\pi$ orbital, is the lowest state of $^1\Pi_g$ symmetry in H_2. It was observed by Dieke in emission to the lower lying $B^1\Sigma_u^+$ and $C^1\Pi_u$ states [82], at the time labeling the excited state as '3E'. Based on *ab initio* calculations by Kolos and Rychlewski [83], Dressler and Wolniewicz calculated diagonal corrections and rovibrational energies [84]. Similarly in the MQDT framework for the gerade states these level energies were calculated as well [20]. The potential, later calculated to higher accuracy [85], is known to exhibit a double well structure, where levels in the outer well $I'^1\Pi_g$ were probed with two-step laser excitation via $B^1\Sigma_u^+$ $v=16$ [56]. The inner well states have been experimentally investigated, also with double resonance laser excitation for the $I^1\Pi_g$, $v=0$ by Tsukiyama *et al.* [38], for the $I^1\Pi_g$, $v=2$ state by Ishii *et al.* [40], and again for $I^1\Pi_g$, $v=0$ by de Lange *et al.* [57]. Yu and Dressler list the values for level energies of $I^1\Pi_g$, $v=0$–3 [19].

In the present FT emission study also the $I^1\Pi_g$, $v=0$–3 levels are probed, and the values are listed in Table 9. Note that for the assignment we have followed Ross and Jungen [20] and Ishii *et al.* [40], which deviates from Yu and Dressler [19], in particular for $I^+(v=2)$. With this assignment, following Figure 6, the Λ-doubling in the $I^1\Pi_g$, $v=2$ state is smallest. The obtained accuracies vary from one to a few times $10^{-3}\,cm^{-1}$. In a comparison with the data (after reassignment) of [19] we find good agreement, with systematically lower term values in the present study by $0.04\,cm^{-1}$, which we consider to be reasonable.

A comparison can be made with the five level energies determined by de Lange *et al.* [57] at an accuracy of $0.006\,cm^{-1}$. The deviation between the values in Table 9 and those of de Lange are $-0.002\,cm^{-1}$, well within the joint uncertainties.

3.9. *The* $J^1\Delta_g$ *state*

The $J^1\Delta_g$ state, associated with a $3d\delta$ orbital, is the lowest state of $^1\Delta_g$ symmetry in H_2. Also for the $^1\Delta_g$ state two Λ-doublet components can be discerned: the $^1\Delta_g^+$ and $^1\Delta_g^-$ component. An *ab initio* calculation for the $J^1\Delta_g$ state was performed by Kolos and Rychlewski [86], and later by Wolniewicz [85]. Similarly MQDT calculations already produced level energies for the $J^1\Delta_g$ state [20]. The level energies of the Dieke atlas are listed in [19].

In the present FT emission spectrum level energies were determined for $J^1\Delta_g$, $v=0$–2, for both $^1\Delta_g^+$ and $^1\Delta_g^-$ components; results are listed in Table 10. The comparison between the data of Table 10 and those of [19] shows the present data to be systematically lower by some $0.03\,cm^{-1}$. For the values obtained by double-resonance laser excitation by Tsukiyama and co-workers [38,40] the agreement is well within the stated uncertainties. The two level energies measured by de Lange *et al.* [57] are, again, well within the stated uncertainty of $0.006\,cm^{-1}$.

3.10. *Updated set of Lyman and Werner lines*

The Lyman and Werner band systems are the strongest absorption systems to monitor the hydrogen molecule. These bands can nowadays be observed in absorption against the dim background emission of highly red-shifted quasars systems. Recently these spectra have been used for detecting possible variations in the proton-electron mass ratio [26,27,87,88]. For this application highly accurate laboratory wavelengths of the Lyman and Werner absorption bands are required, and this formed the major motivation for the present investigation, as was elucidated in the preliminary report [28]. The highly accurate level energies of the

Table 11. Calculated wavelengths (and uncertainties) of the Lyman band lines in the $B^1\Sigma_u^+ - X^1\Sigma_g^+$ band system, with Lv referring to the (v',0) band. Values in nm.

	P(1)		P(2)		P(3)		P(4)	
L0	111.0062558	(3)	111.2495989	(3)	111.5895530	(3)	112.0248839	(3)
L1	109.4051949	(3)	109.6438914	(5)	109.9787177	(5)	110.4083933	(7)
L2	107.8925400	(3)	108.1265950	(4)	108.4560256	(3)	108.8795369	(4)
L3	106.4605318	(4)	106.6900633	(4)	107.0140818	(3)	107.4312899	(5)
L4	105.1032451	(5)	105.3284210	(4)	105.6471373	(3)	106.0580970	(4)
L5	103.8157044	(4)	104.0367202	(3)	104.3503090	(4)	104.7551786	(4)
L6	102.5935181	(6)	102.8105875	(7)	103.1192672	(4)	103.5182762	(5)
L7	101.4327128	(6)	101.6461136	(5)	101.9502139	(3)	102.3436799	(5)
L8	100.3296508	(5)	100.5393086	(5)	100.8386075	(3)	101.2262348	(5)
L9	99.2809625	(4)	99.4874026	(6)	99.7827121	(3)	100.1655682	(5)
L10	98.2835296	(5)	98.4864026	(7)	98.7768823	(4)	99.1533853	(6)
L11	97.3344571	(6)	97.5345771	(8)	97.8218030	(3)	98.1948441	(3)
L12	96.4310524	(6)	96.6275434	(9)	96.9089768	(4)	97.269064	(3)
L13	95.5708153	(9)	95.7652228	(9)	96.0450567	(5)	96.409079	(2)
	P(5)		R(0)		R(1)		R(2)	
L0	112.5540690	(5)	110.81273169	(17)	110.8633244	(3)	111.0120562	(3)
L1	110.9313238	(4)	109.2195201	(4)	109.2732382	(4)	109.4244560	(7)
L2	109.3954976	(3)	107.7138656	(3)	107.7698852	(3)	107.9225425	(4)
L3	107.9400450	(4)	106.2882074	(4)	106.3460086	(3)	106.4994759	(4)
L4	106.5596570	(4)	104.9367383	(4)	104.9959704	(3)	105.1498512	(4)
L5	105.2496918	(4)	103.65456797	(16)	103.7149822	(3)	103.8690179	(3)
L6	104.0059726	(4)	102.4373738	(6)	102.4987976	(3)	102.6528323	(5)
L7	102.8248570	(4)	101.2812914	(4)	101.3436916	(2)	101.4976843	(5)
L8	101.7004186	(5)	100.1823741	(4)	100.2452009	(3)	100.3985377	(5)
L9	100.6343184	(3)	99.1378851	(5)	99.2016320	(2)	99.3550563	(5)
L10	99.6124697	(6)	98.1438709	(7)	98.2074245	(4)	98.3591063	(5)
L11	98.6520717	(4)	97.1986230	(8)	97.2632731	(3)	97.4157875	(2)
L12	97.7463601	(5)	96.2977981	(8)	96.3607928	(3)	96.504571	(3)
L13	96.8556580	(7)	95.4413268	(9)	95.5065759	(5)	95.6579917	(18)
	R(3)		R(4)		R(5)			
L0	111.2583944	(5)	111.6014618	(7)	112.0400623	(5)		
L1	109.6725316	(4)	110.0164528	(7)	110.4548705	(5)		
L2	108.1711274	(3)	108.5145527	(5)	108.9513848	(5)		
L3	106.7478598	(4)	107.0900286	(6)	107.5244947	(6)		
L4	105.3976051	(4)	105.7380706	(7)	106.1697413	(5)		
L5	104.1158832	(4)	104.4543977	(5)	104.8830369	(5)		
L6	102.8986607	(4)	103.2350972	(8)	103.660473	(2)		
L7	101.7424212	(4)	102.0767035	(11)	102.4990170	(11)		
L8	100.6414053	(5)	100.971969	(2)	–			
L9	99.5972783	(3)	99.9270807	(5)	–			
L10	98.5962767	(6)	–		–			
L11	97.6552811	(4)	97.980509	(2)	–			
L12	96.7676976	(5)	97.0838045	(10)	–			
L13	95.8946624	(7)	96.215273	(6)	–			

$B^1\Sigma_u^+$ and $C^1\Pi_u$ rovibronic levels now permit a calculation of transition frequencies, or wavelengths, which are more accurate than the best direct measurements in XUV spectroscopies [10,73,74].

From quadrupole spectroscopy of H_2 [89], highly accurate ground state rotational level energies were determined: $N=1$ at 118.48684 (10) cm^{-1}, $N=2$ at 354.37354 (21) cm^{-1}, $N=3$ at 705.51906 (19) cm^{-1}, $N=4$ at 1168.79827 (22) cm^{-1}, and $N=5$ at 1740.18930 (19) cm^{-1}. In the cold environment of distant galaxies absorbing in the Lyman and Werner band lines only the six lowest rotational ($N=0$–5) states of $v=0$

Table 12. Calculated wavelengths (and uncertainties) of the Werner band lines in the $C^1\Pi_u - X^1\Sigma_u^+$ band system, with Wv referring to the $(v', 0)$ band. Values in nm.

	P(2)		P(3)		P(4)		P(5)	
W0	101.216946	(2)	101.4504259	(5)	101.7385588	(5)	102.0799172	(6)
W1	98.9088421	(9)	99.1380493	(5)	99.4229935	(6)	99.764142	(7)
W2	96.829519	(6)	97.0563360	(7)	97.345239	(2)	97.654879	(3)
W3	94.961045	(3)	95.167184	(1)	95.447400	(5)	95.781887	(3)
	Q(1)		Q(2)		Q(3)		Q(4)	
W0	100.9770899	(6)	101.0938509	(8)	101.2679615	(6)	101.498244	(3)
W1	98.6798049	(8)	98.7974478	(9)	98.9729361	(3)	99.205124	(3)
W2	96.6096120	(7)	96.728107	(3)	96.9049316	(10)	97.138968	(2)
W3	94.7421917	(3)	94.861582	(18)	95.0397767	(18)	95.275740	(6)
	Q(5)		R(0)		R(1)		R(2)	
W0	101.783147	(3)	100.855192	(2)	100.8498181	(5)	100.9024969	(5)
W1	99.492543	(2)	98.5633709	(9)	98.5644316	(4)	98.6244066	(6)
W2	97.428818	(2)	96.498397	(6)	96.5064884	(7)	96.579552	(2)
W3	–		94.642556	(3)	94.6384745	(9)	94.711165	(5)
	R(3)		R(4)		R(5)			
W0	101.0130272	(6)	101.181449	(3)				
W1	98.744868	(7)	98.887151	(4)	99.137172	(5)		
W2	96.678038	(3)	96.866686	(8)	97.107625	(6)		
W3	94.841978	(3)	95.031519	(7)				

are populated. Combining these values with the level energies of the $B^1\Sigma_u^+$ and $C^1\Pi_u$ states (as listed in Tables 5 and 6) yield the highly accurate values for Lyman and Werner lines as calculated and listed in Tables 11 and 12. For convenience of use in astrophysical analysis, the data are given in units of (vacuum) wavelength. With respect to the partial listing in [28], we now extend the data to higher J-values, and include also C ($v = 3$) and B ($v = 13$). The uncertainties in the line wavelengths are derived from the combined uncertainties in the level energies of ground and excited states.

In our preliminary report [28], we have already made a comparison between the newly calibrated data and those obtained from the direct XUV measurements of [10,73,74]. That comparison showed agreement between the data sets to within 2σ and some systematic shift of 1σ in the range of $B^1\Sigma_u^+$, $v = 5$–8. We plot the difference in the transition energies obtained from the present FT-derived and direct XUV data sets, normalised by the combined 1σ uncertainty, against the transition energy of the Lyman transitions in Figure 7(a). We have indicated the P- and R-branches to highlight the common systematic trend of both branches. Figure 7 shows that in certain wavelength ranges there seem to exist systematic shifts even to the 3σ level. We attribute these systematic shifts to be from the XUV data set, specifically to unaccounted frequency chirp shifts which are particularly severe around $97{,}000\,\mathrm{cm}^{-1}$ which are at the edge of the emission curve of the dyes used. It has been shown that the shifts due to chirp effects in pulsed dye amplifiers (PDA) can be large [90,91]. We also plot similar differences for all observed P, Q, and R lines in the Werner bands (occurring at $> 98{,}000\,\mathrm{cm}^{-1}$) in Figure 7(b), where we do not find systematic offsets.

As had been discussed in the context of the direct XUV measurements [10,73,74] the calculated ground state splittings from the combination difference of the respective P and R transitions (in XUV excitation) with a common upper level are more accurate than the transition values since some systematic shifts cancel out, e.g. $\Delta(N = 2 \leftarrow N = 0) = 354.373(3)\ \mathrm{cm}^{-1}$. This cancelling out also holds for the chirp effects, since the combined P and R lines relatively close on the wavelength scale. As a particular example, the XUV determination of P(2), P(3), R(0), and R(1) transitions in the B–X (8,0) Lyman band differ from the FT

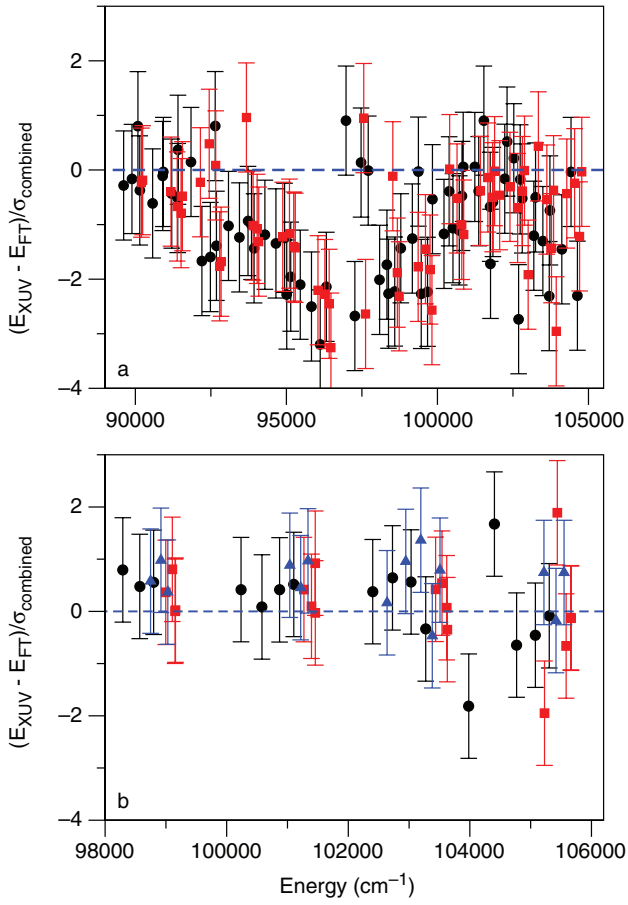

Figure 7. Comparison of the Lyman and Werner transitions derived from the FT data and from direct XUV excitation. The filled circles (•), squares (■) and triangles (▲) indicate transitions belonging to the P-, R- and Q-branch (Werner), respectively. (a) The normalised transition energy differences of the Lyman transitions show severe systematic shifts around 97,000 cm^{-1}, which we attribute to frequency chirp effects in the PDA. (b) Werner transitions (>98,000 cm^{-1}) do not show severe systematic trends.

derived values by as much as 0.012 cm^{-1}. However, the $\Delta(N=2 \leftarrow N=0)$ and $\Delta(N=3 \leftarrow N=1)$ ground state splittings obtained from the respective combination differences agree with the highly accurate results of the far-infrared study [89] to within 0.0016 cm^{-1}. This deviation is much smaller than the estimated uncertainty of 0.005 cm^{-1} for the corresponding direct XUV transition energies.

The present reanalysis of the data after our preliminary report [28] includes additional transitions in the determination of the level energies, while also the statistical averaging procedure was reevaluated. As a result, the values and the estimated uncertainties of the Lyman and Werner transitions presented in Tables 11 and 12 are slightly different but are in agreement with the values in the previous report [28]. The wavelengths listed in Tables 11 and 12 are the recommended data to be used in comparison with quasar data extracting possible variations of the proton–electron mass ratio.

4. Conclusion

In the present study, we have determined accurate level energies of over 500 rovibronic quantum levels in the $EF^1\Sigma_g^+$, $GK^1\Sigma_g^+$, $H^1\Sigma_g^+$, $B^1\Sigma_u^+$, $C^1\Pi_u$, $B'^1\Sigma_u^+$, $D^1\Pi_u$, $I^1\Pi_g$, and $J^1\Delta_g$ excited states of H_2. For some levels with low v and N quantum numbers in the $EF^1\Sigma_g^+$ and $B^1\Sigma_u^+$ states, observed through many lines in several strong systems from which combination differences could be used, term values were determined with an accuracy of 0.001 cm^{-1} or better, while for most of the other levels the accuracy is at several 0.001 cm^{-1}. A comparison is made with previous determinations of the level energies. Comparison with the comprehensive studies on the states of gerade symmetry by Yu and Dressler [19] yield general agreement to within a few 0.01 cm^{-1}. Comparing with the classical VUV work on the states of ungerade symmetry by Abgrall *et al.* [15,25] yields agreement at the level of 0.1 cm^{-1}, which is the estimated accuracy in these classical studies. Next a comparison was made with the laser excitation studies in which commercial pulsed dye lasers were employed [16,17,38,40,80]. Agreement was found at the level of 0.05 cm^{-1} or better, which may be typically expected from such experiments involving pulsed dye lasers.

More stringent constraints on the present data set can be obtained from a comparison with data from studies performed with ultra-narrow bandwidth lasers. Already in the preliminary report [28] a comparison was made between the present data and the direct XUV excitation of the Lyman and Werner bands as in [10,73,74], measured at an accuracy of 0.005 cm^{-1}. As discussed in [28] good agreement was found, except in a certain wavelength range where the $B^1\Sigma_u^+$ ($v=5$–8) levels are excited, somewhat larger discrepancies persist. These discrepancies were attributed to chirp phenomena in the XUV laser setup. A highly accurate assessment of the gerade states is possible through a comparison with the precise two-photon excitation schemes in [57], at the level of 0.006 cm^{-1}, and in the scheme of [66], where a precision of 0.003 cm^{-1} was achieved. Both studies agree well with the present findings.

However, comparisons with previous results are insufficient, since in the present work for some levels an unprecedented accuracy is estimated. For such cases, most notable in the $EF^1\Sigma_g^+$ and $B^1\Sigma_u^+$ states, we have to

rely on the internal consistency of the measurements. These levels were observed in a great number of spectral lines, at widely varying wavelengths, providing a large number of combination differences. The final accuracy is derived from an averaging procedure, and is statistical in nature. There is a further possibility of testing the internal consistency of these methods, and that is based on the levels in the $EF^1\Sigma_g^+$ ($v=0$) state. Whereas the anchor lines are determined as the $N=0$ and $N=1$ levels in $EF^1\Sigma_g^+$ ($v=0$), the results of the $N=2$–5 levels from the FT-spectroscopy can be compared with the results of the direct two-photon excitation of these levels. The discrepancies between the methods are found at the level of $0.00021\,cm^{-1}$, whereas the accuracy of the level energies from the direct deep-UV two-photon studies is at $0.00024\,cm^{-1}$ [28]. This agreement is the most stringent test on the absolute accuracy of those lines in the present data set, for which the accuracy is estimated to be the highest.

Tables 11 and 12 contain the best and most updated values of the Lyman and Werner band wavelengths to be used in probing possible variations of fundamental constants based on the H_2 molecule.

Supplementary material

An electronic database (H_2 rovibronic transitions 2000–22,000 cm^{-1}) containing all analysed transition frequencies of the Fourier transform emission study is available as supplementary material to this paper online.

Acknowledgement

The authors acknowledge financial support from the Netherlands Foundation for Fundamental Research of Matter (FOM). They wish to thank the anonymous referee for valuable comments.

References

[1] H. Cavendish, Trans. Roy. Soc. **56**, 141 (1766).
[2] A. Lavoisier, Observations sur la Physique **23**, 452 (1783).
[3] J.L. Gay-Lussac, Mémoires de la Sociétée d'Arcueil **2**, 207 (1809).
[4] A. Avogadro, J. Phys. (Paris) **73**, 58 (1811).
[5] J.W. Plücker and J. Hittorf, Phil. Trans. Roy. Soc. (London), A **155**, 1 (1865).
[6] G.S. Fulcher, Astroph. J. **34**, 388 (1911).
[7] T. Lyman, Astroph. J. **23**, 181 (1906).
[8] O.W. Richardson, *Molecular Hydrogen and its Spectrum* (Yale University Press, New Haven, 1934).
[9] H.M. Crosswhite, *The Hydrogen Molecule Wavelength Tables of Gerhard Heinrich Dieke* (Wiley–Interscience, New York, 1972).
[10] G. Herzberg and L.L. Howe, Can. J. Phys. **37**, 636 (1959).
[11] I. Dabrowski, Can. J. Phys. **62**, 1639 (1984).
[12] J.-Y. Roncin and F. Launay, J. Phys. Chem. Ref. Data, Monograph **4** (1994).
[13] H. Abgrall, E. Roueff, F. Launay, J.-Y. Roncin, and J.-L. Subtil, Astron. Astroph. Suppl. Ser. **101**, 273 (1993).
[14] H. Abgrall, E. Roueff, F. Launay, J.-Y. Roncin, and J.-L. Subtil Astron, Astroph. Suppl. Ser. **101**, 323 (1993).
[15] H. Abgrall, E. Roueff, F. Launay, J.-Y. Roncin, and J.-L. Subtil, J. Mol. Spectrosc. **157**, 512 (1993).
[16] P.C. Hinnen, W. Hogervorst, S. Stolte, and W. Ubachs, Appl. Phys. B **59**, 307 (1994).
[17] P.C. Hinnen, W. Hogervorst, S. Stolte, and W. Ubachs, Can. J. Phys. **72**, 1032 (1994).
[18] J. Philip, J.P. Sprengers, T. Pielage, C.A. de Lange, W. Ubachs, and E. Reinhold, Can. J. Chem. **82**, 713 (2004).
[19] S. Yu and K. Dressler, J. Chem. Phys. **101**, 7692 (1994).
[20] S.C. Ross and C. Jungen, Phys. Rev. A **50**, 4618 (1994).
[21] P. Senn, P. Quadrelli, and K. Dressler, J. Chem. Phys. **89**, 7401 (1988).
[22] C. Jungen and O. Atabek, J. Chem. Phys. **66**, 5584 (1977).
[23] W. Kolos and L. Wolniewicz, Rev. Mod. Phys. **35**, 473 (1963).
[24] L. Wolniewicz, J. Chem. Phys. **103**, 1792 (1995).
[25] H. Abgrall, E. Roueff, F. Launay, and J.-Y. Roncin, Can. J. Phys. **72**, 856 (1994).
[26] W. Ubachs and E. Reinhold, Phys. Rev. Lett. **92**, 101302 (2004).
[27] E. Reinhold, R. Buning, U. Hollenstein, P. Petitjean, A. Ivanchik, and W. Ubachs, Phys, Rev. Lett. **96**, 151101 (2006).
[28] E.J. Salumbides, D. Bailly, A. Khramov, A.L. Wolf, K.S.E. Eikema, M. Vervloet, and W. Ubachs, Phys. Rev. Lett. **101**, 223001 (2008).
[29] S. Hannemann, E.J. Salumbides, S. Witte, R.T. Zinkstok, E.-J. van Duijn, K.S.E. Eikema, and W. Ubachs, Phys. Rev. A **74**, 062514 (2006).
[30] C. Jungen, I. Dabrowski, G. Herzberg, and D.J.W. Kendall, J. Chem. Phys. **91**, 3926 (1989).
[31] C. Jungen, I. Dabrowski, G. Herzberg, and M. Vervloet, J. Chem. Phys. **93**, 2289 (1990).
[32] D. Bailly and M. Vervloet, Mol. Phys. **105**, 1559 (2007).
[33] S. Hannemann, E.-J. van Duijn, and W. Ubachs, Rev. Sci. Instrum. **78**, 103012 (2007).
[34] S. Hannemann, E.J. Salumbides, and W. Ubachs, Opt. Lett. **32**, 1381 (2007).
[35] The potential energy curves were obtained from the website of Prof. L. Wolniewicz at Torun University: http://www.fizyka.umk.pl/ftp/publications/ifiz/luwo/

[36] A.G. Maki, J.S. Wells, and D.A. Jennings, J. Mol. Spectrosc. **144**, 224 (1990).
[37] G. Norlén, Phys. Scr. **8**, 249 (1973).
[38] K. Tsukiyama, J. Ishii, and T. Kasuya, J. Chem. Phys. **97**, 875 (1992).
[39] K. Tsukiyama, S. Shimizu, and T. Kasuya, J. Mol. Spectrosc. **155**, 352 (1992).
[40] J. Ishii, K. Tsukiyama, and K. Uehara, Laser Chem. **14**, 31 (1994).
[41] E.R. Davidson, J. Chem. Phys. **35**, 1189 (1961).
[42] J. Gerhause and H.S. Taylor, J. Chem. Phys. **42**, 3621 (1965).
[43] W. Kolos and L. Wolniewicz, J. Chem. Phys. **50**, 3228 (1969).
[44] K. Dressler, R. Galluser, P. Quadrelli, and L. Wolniewicz, J. Mol. Spectrosc. **75**, 205 (1979).
[45] L. Wolniewicz and K. Dressler, J. Chem. Phys. **82**, 3292 (1985).
[46] P. Quadrelli, K. Dressler, and L. Wolniewicz, J. Chem. Phys. **92**, 7461 (1990).
[47] P. Senn, P. Quadrelli, K. Dressler, and G. Herzberg, J. Chem. Phys. **83**, 962 (1985).
[48] P. Senn and K. Dressler, J. Chem. Phys. **87**, 6908 (1987).
[49] D.J. Kligler and C.K. Rhodes, Phys. Rev. Lett. **40**, 309 (1978).
[50] E.E. Marinero, C.T. Rettner, and R.N. Zare, Phys. Rev. Lett. **48**, 1323 (1982).
[51] W.L. Glab and J.P. Hessler, Phys. Rev. **A35**, 2102 (1987).
[52] E.E. Eyler, J. Gilligan, E. McCormack, A. Nussenzweig, and E. Pollack, Phys. Rev. **A36**, 3486 (1987).
[53] J.M. Gilligan and E.E. Eyler, Phys. Rev. **A46**, 3676 (1992).
[54] D. Shiner, J.M. Gilligan, B.M. Cook, and W. Lichten, Phys. Rev. **A47**, 4042 (1993).
[55] A. Yianopoulou, N. Melekechi, S. Gangopadhyay, J.C. Meiners, C.H. Cheng, and E.E. Eyler, Phys. Rev. **A73**, 022506 (2006).
[56] E. Reinhold, A. de Lange, W. Hogervorst, and W. Ubachs, J. Chem. Phys. **109**, 9772 (1998).
[57] A. De Lange, E. Reinhold, and W. Ubachs, Phys. Rev. **A65**, 064501 (2002).
[58] L. Wolniewicz and K. Dressler, J. Mol. Spectrosc. **67**, 416 (1977).
[59] L. Wolniewicz and K. Dressler, J. Mol. Spectrosc. **77**, 286 (1979).
[60] L. Wolniewicz and K. Dressler, J. Chem. Phys. **82**, 3292 (1985).
[61] L. Wolniewicz and K. Dressler, J. Chem. Phys. **100**, 444 (1994).
[62] E. Reinhold, W. Hogervorst, and W. Ubachs, Phys. Rev. Lett. **78**, 2543 (1997).
[63] L. Wolniewicz, J. Chem. Phys. **109**, 2254 (1998).
[64] L. Wolniewicz, J. Chem. Phys. **108**, 1499 (1998).
[65] E. Reinhold, W. Hogervorst, W. Ubachs, and L. Wolniewicz, Phys. Rev. **A60**, 1258 (1999).
[66] H.J. Wörner, S. Mollet, Ch. Jungen, and F. Merkt, Phys. Rev. **A75**, 062511 (2007).
[67] W. Kolos, K. Szalewicz, and H.J. Monkhorst, J. Chem. Phys. **84**, 3278 (1986).
[68] J. Liu, U. Hollenstein, F. Merkt, E.J. Salumbides, J.C.J. Koelemeij, K.S.E. Eikema, and W. Ubachs, J. Chem. Phys. **130**, 174306 (2009).
[69] W. Kolos and L. Wolniewicz, Can. J. Phys. **53**, 2189 (1975).
[70] L. Wolniewicz and K. Dressler, J. Chem. Phys. **88**, 3861 (1988).
[71] L. Wolniewicz, J. Chem. Phys. **96**, 6053 (1992).
[72] L. Wolniewicz, Chem. Phys. Lett. **233**, 647 (1995).
[73] U. Hollenstein, E. Reinhold, C.A. de Lange, and W. Ubachs, J. Phys. B **39**, L195 (2006).
[74] T.I. Ivanov, M.O. Vieitez, C.A. de Lange, and W. Ubachs, J. Phys. B **41**, 035702 (2008).
[75] S. Werner, Proc. R. Soc. London Ser. A **113**, 107 (1926).
[76] W. Kolos and J. Rychlewski, J. Mol. Spectrosc. **62**, 109 (1976).
[77] L. Wolniewicz and G. Staszewska, J. Mol. Spectrosc. **220**, 45 (2003).
[78] W. Kolos, J. Mol. Spectrosc. **62**, 429 (1976).
[79] T. Namioka, J. Chem. Phys. **41**, 2141 (1964).
[80] E. Reinhold, W. Hogervorst, and W. Ubachs, J. Mol. Spectrosc. **180**, 156 (1996).
[81] S. Takezawa, J. Chem. Phys. **52**, 2575 (1970).
[82] G.H. Dieke, Z. Phys. **55**, 447 (1929).
[83] W. Kolos and J. Rychlewski, J. Mol. Spectrosc. **66**, 428 (1977).
[84] K. Dressler and L. Wolniewicz, Can. J. Phys. **62**, 1706 (1984).
[85] L. Wolniewicz, J. Mol. Spectrosc. **169**, 329 (1995).
[86] W. Kolos and J. Rychlewski, J. Mol. Spectrosc. **91**, 128 (1982).
[87] W. Ubachs, R. Buning, K.S.E. Eikema, and E. Reinhold, J. Mol. Spectrosc. **241**, 155 (2007).
[88] J.A. King, J.K. Webb, M.T. Murphy, and R.F. Carswell, Phys. Rev. Lett. **101**, 251304 (2008).
[89] D.E. Jennings, S.L. Bragg, and J.W. Brault, Astroph. J. Lett. **282**, L85 (1984).
[90] S. Gangopadhyay, N. Melekechi, and E.E. Eyler, J. Opt. Soc. Am. B **11**, 231 (1994).
[91] K.S.E. Eikema., W. Ubachs, W. Vassen, and W. Hogervorst, Phys. Rev. A **55**, 1866 (1997).